

Analysis and Simulation of Variable Range Hopping Parameters Under Photo-excitation

By
Suha Khaled Tawfeeq Jazzar

A thesis submitted for the partial fulfillment of the degree of
Master of Science

Supervisor

Dr. Abdelhalim Ziqan

Co-Supervisor

Prof. Dr. Atef F. Qasrawi

Department of Mathematics and Natural Sciences
Arab American University-Jenin AAUJ

September, 2014

Analysis and Simulation of Variable Range Hopping Parameters Under Photo-excitation

By

Suha Khaled Tawfeeq Jazzar

This Thesis was defended successfully on 06/09/2014 and approved by:

Committee Members:

Signature

- | | |
|--|-------|
| 1. Dr. Abdelhalim Ziqan (Supervisor) | |
| 2. Prof. Dr. Atef Qasrawi (Co-Advisor) | |
| 3. Dr. Iyad Suwan (Internal Examiner) | |
| 4. Dr. Khaled Elaiwi (External Examiner) | |

An-Najah National University

DEDICATION

**To my father, my mother, my brothers, my sister, and
to all my friends.**

Acknowledgements:

I would like to thank my supervisor Dr. Abdelhalem Zeiqan for his guidance and helpful suggestions throughout this thesis. I also would like expressing my sincere appreciation to my co-advisor Prof. Atef Qasrawi: In the world of strong long range I would be lost without him. Thank you so much for your patience and all the time you spent on widening my horizons, I'll never forget it. Your devotion to the subject has been of a great inspiration. A sincere gratitude to my husband Dr. Orwa, my family and my friends. Thank you all for the moral support, for helping me through the times of frustration, and for your patience.

September, 2014

List of Content

Topic:	Page
Dedication	iii
Acknowledgements	iv
List of Content	v
List of Abbreviation	vii
List of symbols	viii
List of Tables.....	xi
List of Figures	xii
Abstract	xiv
ملخص	xvi
Introduction	1
Chapter 1: Basic concepts	6
1.1 Mathematics Definitions	6
1.1.1 Poisson's Equation	6
1.1.2 Boltzmann Distribution	7
1.2 Physics Definitions	8
1.3 Mott's Formalism	9
1.4 Percolation Theory	10
1.4.1 Formalism Based on Percolation Theory	10
1.4.2 The Mathematics of Percolation	11
1.4.3 Analytical Solutions of the Percolation Problem	12
1.4.4 Numerical Solutions of the Percolation Problem	13
1.5 Hopping Conduction	14
1.5.1 General Definition	14
1.5.2 Variable Range Hopping Conduction	15
1.5.3 Hopping Probabilities	16
Chapter 2: The Derivation of Hopping Theory	17
Chapter 3: Simulation of the Hopping Theory	28
3.1 Analysis of Temperature Regions	28
3.2 Compute the Density of State at Fermi Level	34
3.3 Approach of Mixed Conduction	39

Chapter 4: Results and Discussion (non-constant DOS).....	46
4.1 The Polynomial DOS	46
4.2 The Exponential DOS	55
Conclusion	62
Appendix A: Curve Fitting by Microsoft Excel to Approximate the Value of λ	63
Appendix B: Fitting of Conductions	65
References	69

List of Abbreviations

CG	Coulomb Gap
CI	Coulomb Interaction
VRH	Variable range hopping
DOS	density of state
Si-(NWs)	silicon nanowires
RRAM	random access memory
FeRAM	Ferro-electric random access memory
PCM	phase change memory
Zn: SiO ₂	Zinc silicon dioxide
CPNWs	Conducting polymer nanowires
pH	Hydrogen ion concentration
PANI	polymers polyaniline

List of Symbols

Symbol	Unit	Description
P_{ij}	1	probability of a carrier tunneling from a localized state i to an empty state j
ω_{ij}	ms^{-1}	Hopping rate between two sites
α	cm^{-1}	Inverse localization length
σ_0	Ω/cm	Conductivity prefatory in percolation theory
E_i	eV	Energy at site i
E_j	eV	Energy at site j
R_{ij}	Cm	Distance between site i and j
f_i	1	Occupation probability of site i
f_j	1	Occupation probability of site j
μ_i	eV	Chemical potential at site i
μ_j	eV	Chemical potential at site j
σ_{ij}	Ω/cm	Conductivity between sites i and j
$\Delta\mu$	eV	Voltage drop over a single hopping distance
k_B	J/K	Boltzmann constant
T	K	Temperature
ΔE	eV	Energy drop over a single hopping distance
∇u^2	1	$\nabla u^2 = \left(\frac{\partial^2}{\partial x^2} + \frac{\partial^2}{\partial y^2} + \frac{\partial^2}{\partial z^2} \right) u(x, y, z)$, assume that u is a function of three dimensions then
Γ_{opt}	Cm	Maximum(optimal) hopping distance between two sites

Q	cm^3 / s	the volumetric fluid flow
$\Gamma_{\alpha\beta}$	1	the number of electrons making transition per unit time (hopping rate)
ϵ_{opt}	eV	Maximum(optimal) hopping energy of initial or final site
Z	1	the partition function
N_i	1	occupied set of states i in Boltzmann distribution
N	1	the number of bonds
N_c	1	the number of bonds at threshold (the “critical” number)
F	$(mW.cm^{-2})$	The light intensity
$r_{\alpha\beta}$	Cm	The distance between the localized centers α and β
$N(E_F)$ or $D(0)$	cm^{-3} eV^{-1}	Density of states
E_F	eV	Fermi energy
R_{ij}	Cm	Distance vector between sites i and j
$\epsilon_{\alpha\beta}$	eV	the required energy to move from site α to site β
T_0	K	the characteristic temperature(degree of disorder)
$\lambda = g^4$	1	the percolation constant with g in the range of 2.06-4.2 depending on the $N(E_F)$
f_i	1	the occupation probability of state
Q_t	1	number of traps per unit area are located at site t that have the energy E_t (the total number of occupied trapping state)
V_{V_0}	Cm	the potential of valance band at the center of the Crystallite

LN	1	the number of carrier trapped
$\theta(P)$	1	Percolation probability
P	1	The probability
Z_{ij}	Ω	resistance needed to hop from a localized state i to an empty state j
Z_t	Ω	Starting resistance
$\sim Z_t$	Ω	Minimum resistance
Λ	cm^2 / Ω	the diffusion constant
N_{ph}	1	the phonon occupation number
$f(\varepsilon)$	1	the probability that the energy level ε will be <i>filled</i> by an electron
$f(1 - \varepsilon)$	1	the probability that the energy level ε will be empty

Values of constants

$\lambda \cong 18.1$ is the percolation constant

$\varepsilon = \gamma^{-1} = 5A$ is typical value.

$a = 10.78 \text{ \AA}$ is the hopping distance.

$V_{ph} = 10^{13} s^{-1}$ is the phonon frequency.

$e = 1.6 \times 10^{-19}$ and $k_B = 86.25 \text{ meV}$.

List of Tables

No.	Table	Page
Table 1	values of E_a and σ_0 get from the plot of experimental data of Conductions with different tempreature along the range T(320-270)K indicative for a variable light intensity F.	31
Table 2	values of T_0 and σ_2 get from the plot of experimental data of Conductions with different tempreature along the range T(260-140)K indicative for a variable light intensity $F(mw.cm^{-2})$.	32
Table 3	actual and predicted values of $N(E_f)$ using the two methods .	36
Table 4	values of λ for different light intensity get from fitting.	38
Table 5	values of γ , $(1/\gamma)$ and γR get from the values of λ	39
Table 6	values of E_a and T_0 we get from the fitting plots in Figures B(1-8) (in appendix B) at different light intensity.	41
Table7	The value of E_m with many correlation of fitting between $m(x)$ function in polynomial DOS ($\lim q \rightarrow 0$) and exponential DOS with $E_i = 0.008ev$.	61

List of Figures

No.	Figure	Page
Graph 1(a & b)	Transport electrons and the relation between the number of carrier trapped and the total number of occupied trapping state.	19
Figure 1	The experimental data for Tl_2SSe_2 crystal under various conductivities	29
Figure 2	the Conduction with different temperature along the range T(320-270)K, showing a $\ln\sigma \sim 1/(1000/T)$ dependence, indicative for a variable light intensity $F = 50, 55, 60, 65, 70, 75$ and $80 (mw.cm^{-2})$.	31
Figure 3-a	Conduction with different temperature along the range T(260-140)K, showing $\ln\sigma \sim (T)^{-\frac{1}{4}}$ dependence, with no light intensity (dark).	33
Figure 3-b	Conduction with different temperature along the range T(260-140)K, showing a $\ln\sigma \sim (T)^{-\frac{1}{4}}$ dependence, indicative for a variable light intensity $F = 50, 55, 60, 65, 70, 75$ and $80 (mw.cm^{-2})$.	34
Figure 4	$N(E_f)$ with different intensity light, showing (a) actual points and (b) the predicted values at some value of $\lambda=5.91E+106=$ infinity.	37
Figure 5	with different temperature along the range T dE_a (320-140) K, showing non-linear relation between dE_a (derivative of E_a) and the temperature, indicative for a variable light intensity at values $F = 50-80 (mw.cm^{-2})$.	40
Figure 6	(get from fitting) with different light intensity T_0 F .	42
Figure 7-a	$N(E_f)$ with different light intensity $F (mw.cm^{-2})$.	43
Figure 7-b	R with different light intensity $F (mw.cm^{-2})$.	43
Figure 7-c	W with different light intensity $F (mw.cm^{-2})$.	44
Figure 7-d	γR with different light intensity $F (mw.cm^{-2})$.	44
Figure 8	Plot of the best correlation of $m(x)$ number of conductances between polynomial DOS ($\lim q \rightarrow 0$) and exponential DOS (with $E_m = 0.08ev$ and $E_i = 0.008ev$ attached to the temperature T(10-300).	60

Figure B1	fitting conductivity at dark.	65
Figure B2	fitting conductivity at $F=50 (mW.cm^{-2})$.	65
Figure B3	fitting conductivity at $F=55 (mW.cm^{-2})$.	66
Figure B4	fitting conductivity at $F=60 (mW.cm^{-2})$.	66
Figure B5	fitting conductivity at $F=65 (mW.cm^{-2})$.	67
Figure B6	fitting conductivity at $F=70 (mW.cm^{-2})$.	67
Figure B7	fitting conductivity at $F=75 (mW.cm^{-2})$.	68
Figure B8	fitting conductivity at $F=80 (mW.cm^{-2})$.	68

Analysis and Simulation of Variable Range Hopping Parameters under Photo-excitation

Suha Jazzar

Supervisor: Dr. Abdelhalim Ziqan

August 2014, 80 pages

Abstract

For the purpose of improving the performance of random access memory (RAM) in computers, the electrical current conduction mechanism which is governed by the variable range hopping (VRH) of electrons from one energy state to another distant site of states is reconsidered. Some recent developments that include less energy consumption, shorter time of response and less heating during run process are attained by getting use from the cheap light energy. Photoexcitation of these devices and device related materials have shown that while the variable range hopping parameters like the degree of disorder, average hopping energy, average hopping energy sharply decreases with increasing light intensity, the density of localized energy states (DOS) near Fermi level and average hopping range significantly increases. The increase of DOS with increasing light intensity is very abnormal and makes the use of Mott's variable range hopping theory questionable. The Mott's theory which was derived assuming invariant DOS was simulated to state the reasons for abnormality. In addition the validity of this theory under variable DOS was analytically proved assuming linear variation of DOS with light energy and was also tested against exponential DOS variation. Mathematical analysis of the theory and its testing parameters have shown that the Mott's model for variable range hopping is still applicable even if the DOS is variable function of energy. This study, which is carried for the first time, is supposed to provide an excellent method for increasing the ability of storage in RAM by increasing the density of states that occupy electrons and shorten the response time of the device by increasing the hopping distance and decreasing the hopping energy through the device.

ملخص

بهدف تحسين أداء ذاكرة الوصول العشوائي (RAM) تكون آلية توصيل التيار الكهربائي للإلكترونات من مستوى طاقة معين إلى موقع آخر ذو مستوى آخر للطاقة محددة، وهذا يعتمد على نطاق النقل المتغير للإلكترونات (VRH). مؤخرا هناك بعض التطورات التي تستهلك طاقة أقل، و وقت استجابة أقصر وحرارة أقل خلال عملية التشغيل عن طريق استخدام الطاقة بأقل التكاليف. وقد أظهر تحفيز الفوتونات (Photoexcitation) لهذه الأجهزة و المواد ذات الصلة بها ان قيمة العوامل المتغيرة لنطاق النقل المتغير (VRH) مثل درجة الفوضى، متوسط نقل الطاقة و متوسط نقل الطاقة الحاد تقل عند زيادة شدة الضوء ، بينما كثافة مستوى الطاقة المحدد (DOS) القريب من مستوى فيرمي و المدى المتوسط للنقل تزيد بشكل كبير. هذه الزيادة لكثافة مستوى الطاقة (DOS) مع زيادة شدة الضوء غير طبيعية وتجعل من استخدام نظرية (Mott's) في نطاق النقل المتغير (VRH) مشكوك فيها. ان نظرية (Mott's) والتي تم اشتقاقها سابقا فرضت ان كثافة مستوى الطاقة (DOS) ثابت طبق على نموذج عملي مصغر (محاكاة) على بيانات لتجربة عملية لفحص ما اذا كان هناك قيم لكثافة مستوى الطاقة غير ثابتة في حالات شاذة عن النظرية. بالإضافة الى انه تم اثبات صحة هذه النظرية تحليليا بوجود قيمة متغيرة لكثافة مستوى الطاقة (DOS) على افتراض ان الانحراف لكثافة مستوى الطاقة (DOS) خطي مع طاقة الضوء وتم اختباره أيضا ضد الانحراف الأسي لكثافة مستوى الطاقة (DOS). وقد أظهر التحليل الرياضي للنظرية واختبار متغيراتها أن نموذج (Mott's) لنطاق النقل المتغير (VRH) لا يزال قابل للتطبيق حتى و ان كانت كثافة مستوى الطاقة (DOS) اقتران متغير للطاقة. هذه الدراسة، التي تتم للمرة الأولى، من المفترض أن توفر وسيلة ممتازة لزيادة قدرة التخزين في ذاكرة الوصول العشوائي (RAM) عن طريق زيادة كثافة مستويات الطاقة

التي تشغل الإلكترونات ونجعل زمن الاستجابة للجهاز قصيرا عن طريق زيادة مسافة النقل للإلكترونات وخفض طاقة النقل خلال الجهاز.

Introduction:

In the history of hopping conduction, Conwell is the first one who suggested the idea of hopping in 1956 [1]. The model of the hopping conduction was fruitful since it is the inspiration source of the Variable Range Hopping (VRH) theory of Mott [2]. Mott was one of the first to give a theoretical description of the low temperature hopping conductivity in strongly disordered systems with localized states [3]. In 1969 he introduced the concept of Variable Range Hopping. He shows: How the long jumps govern the conductivity at sufficiently low temperatures. Mott's theory makes the assumption of a constant density of states near the Fermi level; Mott explained the qualitative concept of Variable Range Hopping by phonon assisted tunneling, on which the Miller-Abrahams resistor network model is based.

Similar ideas were independently proposed by Pines and Anderson [4]. Miller and Abrahams developed the hopping rate where the jumps are governed by the phonon assisted tunneling and suggested the random resistor network model to describe the macroscopic hopping transport. Mott performed a further development of the Miller and Abrahams hopping rate and showed that by making a couple of assumptions a universal law for the hopping conductivity can be obtained.

Mott's Variable Range Hopping theory was brought further and adjusted by including Coulomb interactions between the charged particles within the system. When the strong interactions are taken into account, a different situation than what predicted by Mott's law arises. The Coulomb Gap (CG) in the density of states occurs due to the strong Coulomb Interaction (CI) [5] between the electron energy states close to the Fermi level. Hamilton and Pollak [6] were one of the first to consider the non-constant density of states. Their results were later improved by Efros and Shklovskii [7] and give a new

conductivity relation; Efros and Shklovskii introduced Coulomb interactions into Mott's theory, which modify his original results.

Variable range hopping (**VRH**) is a model describing low-temperature conduction in strongly disordered systems with localized charge-carrier states [2]. In general for d-dimensions, (**VRH**) model has a characterize temperature dependence of:

$$\sigma = \sigma_0 e^{-\left(\frac{T_0}{T}\right)^{1/(d+1)}}$$

With optimal energy:

$$\mathcal{E}_{opt} \sim T^{d/(d+1)} \gg T$$

And optimal distance:

$$r_{opt} \sim 1/T^{d/(d+1)} \gg \mathcal{E}$$

And for three-dimensions:

$$\sigma = \sigma_0 e^{-\left(\frac{T_0}{T}\right)^{1/4}}$$

Here, σ is the conductivity, σ_0 is a constant independent of temperature, T is the temperature in Kelvin and T_0 is the degree of disorder of the system(characteristic temperature).

It is interesting to study hopping conductivity at low temperatures because of savings the semiconductor industry could achieve if they were able to replace single crystal devices with glass layers [8]. The hopping conduction was used to develop information about the density of state (DOS) In silicon nanowires Si-(NWs). The (DOS) give on indication about the crystal quality and the electronic conduction type prior to electronic device fabrication [9]. Before developing polycrystalline silicon NWs based

devices, in particular for high-performance electronics applications, a good understanding of electronic materials properties is required. Based on the hopping process between localized states related to the nanowire size dependent defect density within the polycrystalline silicon nanowire, the Carrier transport in materials is a function of temperature and doping level [9]. All of the non-volatile random access memory devices applications including random access memory (RRAM), Ferro-electric random access memory (FeRAM), magnetic random access memory (MRAM), and phase change memory(PCM) run on the principle of hopping conduction. Kai-Huang Chen[10], reported that the hopping conduction between the activation energies of the (RRAM) play the vital role in resistance switching. Bipolar resistance switching characteristics with different compliance currents of Zn: SiO₂ RRAM were thoroughly analyzed. Owing to the increase of current, it became easier for metal ions to form precipitates with larger diameter, which led to the decrease of hopping distance. Conducting polyaniline nanowires have advantages over other metal or semiconducting nanowires for their low cost, ease of synthesis, and for the ability to locally or site-specifically fabricate the nanowires [11]. Conducting polymer nanowires (CPNWs) have recently emerged as an attractive alternative to metal and semiconducting nanowires for their large conductivity change, flexibility, and ease of synthesis [12,13]. Furthermore, the CPNWs can be synthesized site-specifically at the desired location [13]. The polyaniline nanowire-based sensors have been reported to have improved sensitivity and response time due to their nano- scale morphology. Some of the immediate challenges regarding polyaniline nanowires include improving their conductivity in the physiological pH range, preventing or minimizing the conductivity degradation, and minimizing the hysteresis effect. Much work is currently underway to

address these issues with some areas already showing signs of success, and the number of applications for polyaniline nanowires is expected to increase in the future [11]. Among all the conducting polymers polyaniline (PANI) demonstrates outstanding properties due to its environmental stability, redox reversibility, high electrical conductivity and ease of synthesis that drives it towards potential electrical device applications. It is agreed that in most of its applications the behavior of the conductivity is a long-standing problem. The improvement on electrical properties of doped PANI reflecting the conditions of preparation/dopant incorporation is of fundamental importance [14, 15].

Spinel compounds are being extensively studied for their applications in dew sensors, pigments for protective coatings etc. [16]. These materials find wide industrial applications in dew sensors, pigments for protective coatings and principally for their dielectric properties in chip capacitors, high frequency capacitors and temperature compensating capacitors and in the composition of binders by increasing the flexural strength [17]. The properties of these materials are highly dependent on the structural disorder arising from synthesis procedure and sintering temperature [18]. The electrical property varies from an insulating to a conducting regime [19]. Hence, it results in a wide range of conductivity values. Various charge transport mechanisms have been proposed depending on the conductivity behavior of ceramics with various parameters such as temperature, pressure and doping.

In the light of the above reported remarkable considerations about the hopping transport applications, here in this thesis we will review the derivation and we will simulate the variable range hopping transport theory in the dark and under photoexcitation effect. Particularly, the values of Mott's parameters will be recalculated for each of the applied

illumination intensities. In addition, the Mott's theory will be tested against variable density of localized states.

Chapter One

Basic concepts

This chapter contains five sections. In section one, we give some basic top mathematical definitions that play a pivotal role in the derivation and existing hopping theory and in simulation data for hopping variable parameters like Poisson's Equation, Boltzmann statistics and Gamma Function. And in section two, we explain some physics definitions that are used in our study. In section three, we show the Mott's formalism which developed by Mott the hopping process. In section four, we talk about percolation theory and the analytical and numerical solution percolation problem that are used in the derivation of Mott's hopping theory that based on the thermal energy of electron under constant electric field. Finally, in section five, we discuss hopping conduction, which help us to understand the hopping theory and the Variable Range Hopping conduction (VRH).

1.1 Mathematics definitions:

1.1.1 Poisson's Equation

Poisson's equation is derived from Coulomb's law and Gauss's theorem. In mathematics, Poisson's equation is a partial differential equation with broad utility in electrostatics, mechanical engineering, and theoretical physics [20]. The Poisson equation is:

$$-\nabla^2 u = f \quad (1.1)$$

It is the simplest and the most famous elliptic partial differential equation. The function f is given on two or three dimensional domain and called "source term",

and is often zero, either everywhere or at some specific region (maybe only specific points). In this case, the previous equation called Laplace's equation, results:

$$-\nabla^2 u = 0 \quad (1.2)$$

1.1.2 Boltzmann distribution [21,22]

Boltzmann distribution is a probability measure for the distribution of the states of a system it is also known as the Gibbs measure. The Boltzmann distribution has many applications in many sites where magnitudes of normal variables are important, spatially, in physics. A special case of the Boltzmann distribution is Maxwell–Boltzmann distribution, mathematically, is the distribution of the magnitude of a three-dimensional random vector whose coordinates are independent (identically distribution) that means there is no normal variables. In physics, Maxwell–Boltzmann distribution gives the distribution of speeds of molecules in thermal equilibrium, for example describing the velocities of particles of gas. The Boltzmann distribution for the fractional number of particles N_i / N occupying a set of states i is:

$$\langle N_i \rangle = \frac{g_i}{\exp\left(\frac{E_i - \mu}{kT}\right)} = \frac{N}{Z} g_i \exp\left(\frac{-E_i}{kT}\right) \quad (1.3)$$

where: E_i the i -th energy level, k is the Boltzmann constant, g_i is the degeneracy of energy level i , μ is the chemical potential, T is absolute temperature (assumed to be a well-defined quantity), N is the total number of particles with property $N = \sum_i N_i$, Z is the partition function.

Where:

- I. The partition function is a special case of a normalizing constant in probability theory, in physics, describes the statistical properties of a system in thermodynamic equilibrium.
- II. The degeneracy meaning: the number of states having energy E_i .

The Boltzmann distribution applies only to particles with temperature is high enough and low enough density

1.2 Physical Definitions :

Crystallites : are small, often microscopic crystals that, held together through highly defective boundaries, constitute a polycrystalline solid. Metallurgists often refer to crystallites as grains.

The Fermi level (or Fermi energy) [27]: is the level where the occupancy of electron is 1/2 and it is the total chemical potential for electrons (or electrochemical potential for electrons) and its energy usually denoted by μ or E_F . The Fermi level is denoted by $f(E)$

$$f(E) = \frac{1}{1 + \exp\left(\frac{E - E_f}{k_B T}\right)} = \frac{1}{1 + \exp\left(\frac{E_f - E_f}{k_B T}\right)} = \frac{1}{1 + \exp(0)} = \frac{1}{2}$$

Here: k_B is Boltzmann constant, T is the temperature in Kelvin and E_F is the energy at Fermi level.

The Fermi level of a body is a thermodynamic quantity, and its significance is the thermodynamic work required to add one electron to the body (not counting the work required to remove the electron from wherever it came from). A precise understanding of the Fermi level—how it relates to electronic band structure in determining electronic

properties, how it relates to the voltage and flow of charge in an electronic circuit—is essential to an understanding of solid-state physics.

Thermionic emission: is the **emission** or heating a conducting body to a sufficiently high temperature, electrically charged particles are emitted from it and may be drawn off by a suitable electric field [28]. The particles may be either electrons or ions, according to the nature of the emitter and the prevailing conditions. This occurs because the thermal energy given to the carrier overcomes the binding potential, also known as work function of the metal.

1.3 Mott's Formalism

In the formalism developed by Mott [2], the hopping process is even more simple (or can be simplified) by assuming that the dominant contribution to the hopping current is through states within $k_B T$ of the chemical potential μ , thereby eliminating the exact occupation probabilities of the states in the description. In this case the hopping probabilities are derived directly from the equation:

$$w_{ij} = Y \exp(-2\alpha|R_{ij}|) \left(\exp\left[-(E_i - E_j)/k_B T\right] - 1 \right)^{-1}, \quad (1.7)$$

With the distance hop R_{ij} , and the energy hop w_{ij} . So the probability of a carrier tunneling P_{ij} from a localized state i with energy E_i to an empty state j with energy E_j giving as:

$$P_{ij} \approx \begin{cases} \exp(-2\alpha R_{ij} - \frac{E_j - E_i}{k_B T}) & \text{if } , E_j > E_i \\ \exp(-2\alpha R_{ij}) & \text{if } , E_j \leq E_i \end{cases} \quad (1.8)$$

Where equation (1.8) follow the condition $|E_i - E_j| \geq k_B T$. Since hopping probability depends on both the spatial and energetic separation of the hopping sites it is natural to describe the hopping processes in a four-dimensional hopping space, with three spatial coordinates and one energy coordinate. Hopping probability and hops to sites that are further away in space but closer in energy might be preferable. This is the Variable Range Hopping (**VRH**) process, which concept was introduced by Mott in 1968 [2].

1.4 Percolation Theory

Percolation theory is a branch of probability theory dealing with properties of random media. Originally conceived as dealing with crystals, mazes and random media in general, it now appears in such fields as petroleum engineering, hydrology, fractal mathematics, and the physics of magnetic induction and phase transitions. As explained by the originators of percolation theory [29].

1.4.1 Formalism Based on Percolation Theory

In modeling the (**VRH**) conduction mechanism, a set of sites is supposed to form a random resistors network, with impedances connecting all individual sites given by the inverse of the corresponding hopping probabilities equation (1.8):

$$Z_{ij} \propto \exp(R_{ij}) , \quad (1.9)$$

The basic difficulty in quantitatively describing the overall impedance of this network

in an analytical expression arises from the wide exponential spread in magnitude of the site-to-site resistors between randomly chosen hopping sites. Whereas this wide spread is preventing the use of analytical averaging, it has proven to be helpful when transaction with the problem using a numerical approach based on percolation theory. Following this theory the network is characterized by a sub-set of interconnected sites, spanning the entire volume, with two-site connections $Z_{ij} \leq \tilde{Z}_t$, where Z_t is the starting resistance and \tilde{Z}_t is the minimum resistance needed to include an infinitely large cluster of interconnected sites within an infinitely large network. Essentially, the percolation starting describes the highest impedance of the most conducting percolation path through the system. The actual sub-set of sites participating in the conduction is expected to be, a little bit, bigger than the most conducting percolation path, including more parallel paths with little higher resistance. The overall resistance of the system is described through the optimality of the most conductive percolation path with starting resistance Z_t and a little larger sub-set of sites with – sometimes- a little larger site-to-site resistance.

1.4.2 The Mathematics of Percolation

Percolation theory and its variants can be considered as part of a general framework of statistical theories that deal with structural and transport properties in porous media [30]. Percolation properties is the properties of a macroscopic system that are emerge at the onset of macroscopic connectivity within it, and to understand the concept of connectivity, consider the square lattice, for example, in terms of bond percolation. The (connected) network of bonds is fully saturated and conducts a fluid, and bonds are randomly removed from the network, the intensity of flow between

opposing sides of the network decreases. At one side of the domain, the number of removed bonds by monitoring the fluid flows. In particular, it is of interest to know the number of bonds that must be removed (randomly) in order for no fluid to arrive at the side of the domain. The answer to the question is given by what is known as the percolation threshold. If the number of bonds is denoted by NN , and their number at the threshold is N_c (the “critical” number), one can show [31,32] that the volumetric fluid flow Q , will be determined by a power law of the form:

$$Q \propto (N - N_c)^k \quad (1.10)$$

Where k is some critical exponent that can be found by many ways: theoretical way, computer simulation and/or experiment. Such a simple law holds for N relatively close to N_c .

1.4.3 Analytical Solutions of the Percolation Problem

Percolation in a system is defined as a closed path between two opposite sides of the system. And it concerns the movement and filtering of fluids through porous materials. Recent applications include for example percolation of water through ice, which is important for the melting of the ice caps.

In general percolation theory the criterion of percolation is often expressed in terms of an expected number of connections to a single site needed to ensure a percolating cluster through the system. As in the analytical descriptions, these studies primarily focused on the qualitative relations between the parameters in the system. Although this more analytical approach has proven to be successful in describing the (VRH) process in the Ohmic low-field regime, the convolution of the hopping process into a standard

percolation problem appears less straightforward in the medium-field and the high-field regime, and the charge carriers in the low-field regime are thermally activated [33]. The differences between ‘standard’ percolation solutions and the hopping process appear to concentrate on two issues, often referred to as the concepts of ‘directional constraints’ and ‘correlation between consecutive hops’.

1.4.4 Numerical Solutions of the Percolation Problem

Let us explain the mathematical setting. Percolation is a simple probabilistic model exhibits a phase transition. The simplest version of percolation which takes its place on Z^2 , which is with edges between neighboring vertices. All edges of Z^2 are, independently of each other, chosen to be open with probability P and closed with probability $1 - p$. A basic question in this model is “ what is the probability that there exists an open path from the origin to the square $S_n = [-n, n]^2$? “ a limit as $n \longrightarrow \infty$ of the question raised above is “ what is the probability that there exists an open path from zero to infinity? “ this probability is called the percolation probability is denoted by $\theta(P)$. Clearly $\theta(0) = 0$ and $\theta(1) = 1$, since there are no open edges at all when $P = 0$ and all edges are open when $P = 1$. For some models there is a probability P_c such that $0 < P_c < 1$ which is the global behavior of the system is quite different for $P < P_c$ and for $P > P_c$. Such a sharp transition in global behavior of a system at some parameter value is called a phase transition or a critical phenomenon, and the parameter value at which the transition takes place is called a critical value [34,35].

The basic mathematical methods and techniques of random processes and the overview of the most important applications will make the student using the analytical

techniques easily and models to study questions in modern applications in biology, physics, communication networks, financial market and decision processes.

1.5 Hopping Conduction:

1.5.1 General definition

Hopping Conduction is defined as electric conduction in which the carrier transport is via electrons hopping from one localized state to another. Electron transport through localized state (deep-level state) within the bandgap of a semiconductor includes:

- 1- Electron hops from a state to another state that has a higher energy. A thermal energy is required for this move. This process is thermally assisted tunneling. It depends on temperature.
- 2- Electron hops from a state to another state that has equal energy. This transport is tunneling process. It does not depend on temperature.
- 3- Electron hops from a state to another state that has a lower energy. This transport is tunneling process with the emission of a phonon(s). It does not depend on temperature.

The necessary conditions for the occurrence of hopping are:

- 1- Wave functions of the two localized states must overlap.
- 2- Occupied and empty states must be present for the hopping to occur. This condition make hopping should happen between states that are close to the Fermi level.
- 3- Electron hopping from one localized state to another with a higher energy level needs energy.

1.5.2 Variable Range Hopping Conduction [2,7,36]

When the temperature is very low, the probability of the electron thermal activation between states that are close in space but far in energy becomes smaller than that of electron hopping between some more remote states where they have new energy levels are very close to each other, in this case the characteristic hopping length increases and the temperature decreasing. This kind of hopping called variable range hopping (VRH), in 1968 Mott introduced this concept of a type of hopping conduction (VRH) [2], and Mott's law describes the temperature dependence of the conductivity as following:

$$\sigma = \sigma_0 e^{-\left(\frac{T_0}{T}\right)^4} \quad (1.11)$$

Where: σ_0 is a constant independent of temperature, T is temperature and T_0 is the characteristic temperature, such that:

$$T_0 = \left(\frac{\lambda}{\xi^3 k N(E_F)} \right) \quad (1.12)$$

With k being the Boltzmann constant, $N(E_F)$ being the density of localized states near the Fermi level E_F calculating by adjusting the parameter electronic wave decay length $\xi = \alpha^{-1}$ for localized states ($0.3nm \leq \xi \leq 3nm$) and $\lambda = g^4$ being a constant and g in the range of 2.06-4.2 depending on the $N(E_F)$ feature [9,37]. The average hopping length R is a function of temperature and follows:

$$R \approx d_0 \left(\frac{T_0}{T} \right)^{\frac{1}{4}} \quad (1.13)$$

Where: d_0 is a constant and observed $R \sim T_0^{-\frac{1}{4}}$ dependence. The average hopping length is on the order of the average distance between localized states, and does not vary with temperature.

1.5.3 Hopping Probabilities [47]

If we assume there are no correlations between the occupation probability of different localized states, then the net electron flow between these states is given by:

$$I_{ij} = f_i(1 - f_j)w_{ij} - f_j(1 - f_i)w_{ji} , \quad (1.14)$$

Where: f_i is the occupation probability of state i and w_{ij} is the electron transition rate of the hopping process between the occupied state i to the empty state j .

The occupation probability f_i is given by the Fermi-Dirac distribution function, with chemical potential μ_i at the position of state i , as following:

$$f_i = [\exp[(E_i - \mu_i)/k_B T] + 1]^{-1} , \quad (1.15)$$

The transition rate w_{ij} is related to a hopping probability P_{ij} by

$$w_{ij} = YP_{ij} , \quad (1.16)$$

Where: P_{ij} the probability of success in a hopping attempt between states i and j and Y an unknown parameter related to a certain ‘attempt-frequency’.

Chapter Two

The Derivation of Hopping theory

In this chapter we have three sections, section one is about the derivation of thermionic by using Poisson equation in one dimension and The relation between the number of carrier trapped and the total number of occupied trapping steady, and in section two we work on resistance since Miller and Abbraham proposed a random resistance in which $R_{\alpha\beta}$ connect a pair of vertices, and in last section three we Derive the hopping conductivity.

Derivation of Thermionic Function [48]

Materials are supposed to be created from crystallites of irregular shapes. If material is polycrystalline then crystallites are identical with size L . They are assumed the exhibit the same type of conductivity. The charge carrier distribution is uniform with concentration equal N . The crystallite boundary has no thickness compared to L and contains Q_t of traps per unit area are located at site t that have the energy E_t with respect to intrinsic Fermi level E_F . Traps are initially neutral and become charged by trapping carriers.

The original Mott paper introduced simplifying assumptions that the hopping energy depends inversely on the cube of the hopping distance (in the three dimensions case). Later it was shown that this assumption was unnecessary, and this is proved [38]. And also in the original Mott paper the hopping probability at a given temperature was

depended on two parameters, R the spatial separation of the sites, and E_f , their energy separation.

Transport properties in one dimension

We start with Poisson equation: $\frac{d^2V}{dX^2} = \frac{qN}{\epsilon}$ (2.1)

Where ϵ : dielectric permittivity and $\frac{l}{2} < |X| < l$.

If we integrate equation (2.1) twice and assume that $\frac{dV}{dX} = 0$ at $X = l$ and the

charge carries in the region $(\frac{l}{2}, l)$ are trapped, then

$dV = \left(\frac{qN}{\epsilon} X + V_0 \right) dx$ And by using the boundary condition (BC) we get

$$V_0 = -\frac{qN}{\epsilon} l$$

So; $dV = \left(\frac{qN}{\epsilon} X - \frac{qN}{\epsilon} l \right) dx$

Then, $V(x) = \int \left(\frac{qN}{\epsilon} X - \frac{qN}{\epsilon} l \right) dx = \frac{qN}{2\epsilon} X^2 - \frac{qN}{\epsilon} lX + V_{V_0}$

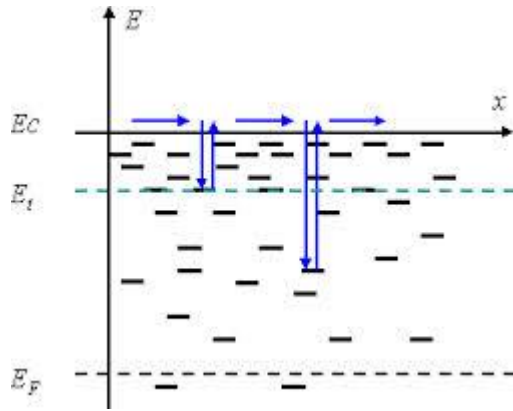
Where: V_{V_0} is the potential of valance band at the center of the Crystallite.

Here $E_{F_i} = 0$ and $E =$ positive value toward valance band.

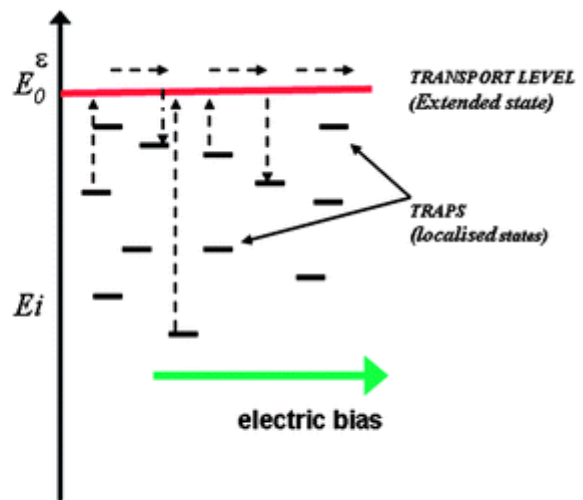
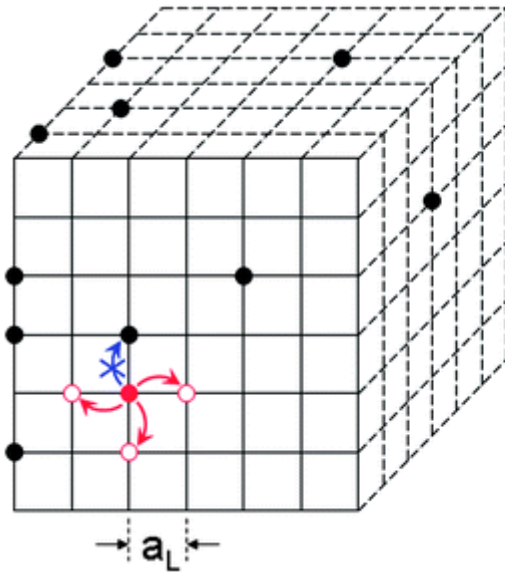
Now we study the relation between the number of carrier trapped and the total number of occupied trapping state.

There are *two* possible conditions: First, $LN < Q_t$, second, $LN > Q_t$,

where LN is the number of carrier trapped and Q_t is the total number of occupied trapping state (see Graphs 1-a&b).



Graph 1-a



Graph 1-b

Case.1 $LN < Q_t$: traps are partially filled where $l = 0$

$$V(X) = \frac{qN}{2\varepsilon} X^2 + V_{V_0}, \quad |X| \leq \frac{l}{2}$$

The potential barrier height is:

$$V_B = V(0) - V\left(\frac{l}{2}\right)$$

$$|V_B| = \left| V_{V_0} - \frac{qN}{2\varepsilon} \frac{l^2}{4} - V_{V_0} \right| = \frac{qN}{8\varepsilon} l^2$$

By Boltzmann statistics, the charge carries are given by the following equation:

$$P(x) = N_V \exp\left(\frac{-qV(x) - E_f}{kT}\right), \quad \varepsilon = qV(x) \text{ and } \mu = E_f$$

Where N_V is the density of states DOS at value bound, k is Boltzmann's constant, $8,62 \times 10^{-5} [eV / K]$.

$$P_a = \left(\int_{-\frac{l}{2}}^{\frac{l}{2}} P(x) dx \right) / L$$

$$P_a = \left(\int_{-\frac{l}{2}}^{\frac{l}{2}} P(x) dx \right) / L = \left(\int_{-\frac{l}{2}}^{\frac{l}{2}} N_V \exp\left(\frac{-q\left(\frac{qN}{2\varepsilon} X^2 + V_{V_0}\right) - E_f}{kT}\right) dx \right) / L$$

We let: $qV_{V_0} = E_B$

$$P_a = \frac{N_V}{L} e^{\frac{-E_B - E_f}{kT}} \int_{-\frac{l}{2}}^{\frac{l}{2}} e^{\frac{-q^2 N}{2\varepsilon kT} X^2} dx = \frac{n_i}{L} \int_{-\frac{l}{2}}^{\frac{l}{2}} e^{\frac{-q^2 N}{2\varepsilon kT} X^2} dx \quad (2.2)$$

Integrate equation (2.2) by using gamma function at 1/2, we get:

$$P_a = \frac{n_i}{Lq} \left(\frac{2\epsilon\pi kT}{N} \right)^{\frac{1}{2}}$$

Where $n_i = N_v e^{\frac{-E_B - E_f}{kT}}$ is the intrinsic carrier density, and intrinsic means :

number of electrons above E_f = number of electrons below E_f , to find E_f must

be the number of carrier trapped = the total number of occupied trapping steady:

$$LN = \frac{Qt}{2e^{\frac{E_t - E_f}{kT}} + 1}$$

$$2e^{\frac{E_t - E_f}{kT}} = \frac{Qt}{LN} - 1$$

$$\frac{E_t - E_f}{kT} = \ln \left(\frac{1}{2} \left(\frac{Qt}{LN} - 1 \right) \right)$$

$$E_f = E_t - kT \ln \left(\frac{1}{2} \left(\frac{Qt}{LN} - 1 \right) \right) \quad (2.3)$$

Case.2 $LN > Q_t$: $l > 0$, part of the crystallite is depleted.

$$V(X) = \frac{qN}{2\epsilon} (X - l)^2 + V_{V_0}$$

$$V\left(\frac{l}{2}\right) = \frac{qN}{8\epsilon} l^2 + V_{V_0}$$

$$V_B = \frac{q}{8\epsilon N} Qt^2$$

In the undeleted region $P_b = N_v \exp \left(\frac{-E_{V_0} - E_f}{kT} \right)$

$$P(x) = N_V \exp\left(\frac{-qV(x) - E_f}{kT}\right)$$

$$P_{avg} = P_b \left(\left(1 - \frac{Qt}{LN}\right) + \frac{1}{qL} \left(\frac{2kT\epsilon \pi}{N}\right)^{\frac{1}{2}} \right)$$

$$J = qP_a V_d = \frac{q^2 P_a E}{m_e}$$

Where V_d : drift velocity, velocity of particles in electric field, and $V_d = \mu E$, here μ is the electron mobility and E is the magnitude of the electric field.

$$J_{th} = qP_a \left(\frac{kT}{2m\pi}\right)^{\frac{1}{2}} e^{\frac{-qV_B}{kT}} \left(e^{\frac{qV_a}{kT}} - 1\right), \text{ Where } qV_a \ll kT$$

$$J_{th} = q^2 P_a \left(\frac{1}{2mkT\pi}\right)^{\frac{1}{2}} e^{\frac{-qV_B}{kT}} V_a$$

$$J = \sigma E \quad \text{and} \quad E = \frac{V}{L} \quad \text{So, } \sigma = \frac{J_{th} L}{V}$$

$$\sigma = Lq^2 P_a \left(\frac{1}{2mkT\pi}\right)^{\frac{1}{2}} e^{\frac{-qV_B}{kT}}$$

$$\sigma \propto e^{\frac{E_t - E_f}{kT}} \quad \text{So, } \sigma \propto \frac{1}{\sqrt{T}} e^{\frac{-E_B}{kT}}$$

Conductivity is evaluated using model of random resistors network proposed by Miller and Abrahams. Considering an elementary hopping process from $\langle \alpha \rangle$ to $\langle \beta \rangle$

when the state energies $E_\alpha \neq E_\beta$. The hopping of electrons (e^-) is accompanied by phonon absorption or emission for the electrons conservation, the number of electrons making transition per unit time (hopping rate) $\Gamma_{\alpha\beta}$ [39]. To move from site α to site β the required energy is $\varepsilon_{\alpha\beta}$ and assumes that the particle successfully reached β .

$$\Gamma_{\alpha\beta} = V_{ph} e^{\frac{-2r_{\alpha\beta}}{\xi}} N_{ph}(\Delta E) f(\varepsilon_\alpha) f(1 - \varepsilon_\beta) \quad (2.4.1)$$

In the case the phonon absorption $\Delta E = \varepsilon_\beta - \varepsilon_\alpha > 0$. Here $r_{\alpha\beta}$ is the distance between the localized centers α and β , $f(\varepsilon)$ is the probability that the energy level ε will be *filled* by an electron and $f(1 - \varepsilon)$ is the probability that the energy level ε will be empty. $N_{ph}(\Delta E)$ and $f(\varepsilon)$ are distribution functions.

$$\Gamma_{\alpha\beta} = V_{ph} e^{\frac{-2r_{\alpha\beta}}{\xi}} [N_{ph}(\Delta E) + 1] f(\varepsilon_\alpha) f(1 - \varepsilon_\beta) \quad (2.4.2)$$

With phonon emission $\Delta E < 0$.

$$N_{ph}(\Delta E) = \frac{1}{e^{\frac{\Delta E}{kT}} - 1} \quad (\text{Boson distribution function}) \quad (2.5)$$

N_{ph} is the phonon occupation number, phonon is mechanical vibration of atom at equilibrium position.

$$f(\varepsilon) = \frac{1}{e^{\frac{\varepsilon}{kT}} + 1} \quad (\text{Fermion distribution function}) \quad (2.6)$$

The localized length is independent from state energy so the transfer integral between

the two states give the factor $e^{\frac{-2r_{\alpha\beta}}{\xi}}$, and by inserting equation (2.5) and equation (2.6) into equation (2.4), the hopping rate become :

$$\Gamma_{\alpha\beta} = V_{ph} e^{\frac{-2r_{\alpha\beta}}{\xi}} e^{\frac{-\varepsilon_{\alpha\beta}}{kT}} \quad (2.7)$$

V_{ph} related to the product of the square of electrons - phonon, matrix element and the density of states (DOS) of phonons V_{ph} depends on $r_{\alpha\beta}$ in weaker than $e^{\frac{-2r_{\alpha\beta}}{\xi}}$ "no spin effect".

$$kT \ll |\varepsilon_{\beta} - \varepsilon_{\alpha}|, \quad kT \ll |\varepsilon_{\beta}| \quad \text{and} \quad kT \ll |\varepsilon_{\alpha}|.$$

$$\text{Where :} \quad \varepsilon_{\alpha\beta} = \frac{|\varepsilon_{\alpha} - \varepsilon_{\beta}| + |\varepsilon_{\alpha}| + |\varepsilon_{\beta}|}{2}$$

And $\varepsilon_{\alpha\beta} = |\varepsilon_{\alpha} - \varepsilon_{\beta}|$ when ε_{α} and ε_{β} lie on opposite site of ε_f

The Resistance of Hopping

The resistance is the ratio of the potential difference across conductor to the current in the conductor: $R = \frac{V}{I}$ (the unit is ohm (Ω) which is one volt per ampere).

$$R_{\alpha\beta} = \frac{kT}{e^2 \Gamma_{\alpha\beta}} = \frac{kT}{e^2 V_{ph}} e^{\left(\frac{2r_{\alpha\beta}}{\xi} + \frac{\varepsilon_{\alpha\beta}}{kT}\right)} \quad (2.8)$$

Miller and Abraham proposed a random resistance network in which $R_{\alpha\beta}$ connect a pair of vertices. The conductivity of the whole system is determined by a set of $\{R_{\alpha\beta}\}$.

The network is extremely wide spectrum of resistance $R_{\alpha\beta}$ due to the exponential depends on $r_{\alpha\beta}$ and $\mathcal{E}_{\alpha\beta}$ when T is not too low ($r_{\alpha\beta}$ dominate) [7]. The electrons hop from localized state to nearest neighborhood state with smallest $r_{\alpha\beta}$, so the temperature dependence in equation (2.8) result in activation type of conductivity :

$$\sigma = \sigma_3 e^{\frac{-\mathcal{E}_3}{kT}}$$

The nearest neighborhood hopping \mathcal{E}_3 is can be evaluated by using the percolation method.

There are two competing factors in the hopping rate; a larger hopping distance $r_{\alpha\beta}$ enables us to find a state with smaller $\mathcal{E}_{\alpha\beta}$ but large $r_{\alpha\beta}$ result in a smaller transfer integral at the same time. The average hopping distance \bar{r} turn out to be $\bar{r} \propto T^{-\frac{1}{4}}$ which leads the hopping conductivity $\sigma = \sigma_0 e^{-\left(\frac{T_0}{T}\right)^{\frac{1}{4}}}$ (variable range hopping).

Take intuitive derivation of equation (2.8) so the problem is to find the optimized hopping distance r that minimizes $\Gamma_{\alpha\beta}$.

Let the **DOS** at the Fermi level be $D(0)$ and the region be the sphere with radius r then the average hopping rate takes the form:

$$\mathcal{E}_{\alpha\beta} = \frac{1}{\frac{4\pi}{3} r^3 D(0)},$$

Substituting equation (2.8) into equation (2.7) we get the following:

$$\Gamma = V_{ph} \exp\left(\frac{-2r}{\xi} - \frac{1}{kT} \frac{3}{4\pi r^3 D(0)}\right) \quad (2.9)$$

Then we take the derivative of Γ with respect to r . But first let:

$$a = \frac{2}{\xi} \quad \text{and} \quad b = \frac{3}{4\pi kTD(0)} \quad \text{then equation (2.9) becomes:}$$

$$\Gamma = V_{ph} e^{-ar} e^{-\frac{b}{r^3}}$$

$$\text{So, } \frac{\partial \Gamma}{\partial r} = V_{ph} \left(-ae^{-ar} e^{-\frac{b}{r^3}} + \frac{3b}{r^4} e^{-ar} e^{-\frac{b}{r^3}} \right) = -V_{ph} \left(a - \frac{3b}{r^4} \right) e^{-\left(ar + \frac{b}{r^3} \right)}$$

To minimize Γ we suppose that $\frac{\partial \Gamma}{\partial r} = 0$ so:

$$-V_{ph} \left(a - \frac{3b}{r^4} \right) e^{-\left(ar + \frac{b}{r^3} \right)} = 0 \quad \text{then we get} \quad r^4 = \frac{3b}{a} = \frac{9\xi}{8\pi kTD(0)}$$

$$\text{So,} \quad R^2 = r^2 = \left(\frac{9\xi}{8\pi kTN(E_f)} \right)^{\frac{1}{2}} \quad (2.10)$$

$$\text{And} \quad W = \varepsilon = \frac{1}{\frac{4\pi}{3} r^3 D(0)} = \frac{3}{4\pi R^3 N(E_f)} \quad (2.11)$$

Replace the value of R in equation (2.11) as value of equation (2.10) to get:

$$W = \varepsilon = \frac{3}{4\pi \left(\frac{9\xi}{8\pi kTN(E_f)} \right)^{\frac{3}{4}} N(E_f)} = \left(\frac{3^4 \times 8^3 \pi^3 k^3 T^3 N^3(E_f)}{4^4 \times 9^3 \xi^3 \pi^4 N^4(E_f)} \right)^{\frac{1}{4}}$$

$$W = \varepsilon = \left(\frac{2k^3 T^3}{9\xi^3 \pi N(E_f)} \right)^{\frac{1}{4}} \quad (2.12)$$

By equation (2.9) we know that $\Gamma = V_{ph} e^{-Y}$ where $Y = \left(\frac{2r}{\xi} + \frac{\varepsilon}{kT} \right)$. Then

from equations (2.10) and (2.12) and simple calculations we have:

$$Y = \left(\frac{2}{\xi} \left(\frac{9\xi}{8\pi kTN(E_f)} \right)^{\frac{1}{4}} + \frac{1}{kT} \left(\frac{2k^3 T^3}{9\xi^3 \pi N(E_f)} \right)^{\frac{1}{4}} \right)$$

$$Y = \left(\frac{2 \times 9^2 + 2}{9\xi^3 \pi kTN(E_f)} \right)^{\frac{1}{4}} \approx \left(\frac{1}{T} \right)^{\frac{1}{4}} \left(\frac{1}{\xi^3 kN(E_f)} \right)^{\frac{1}{4}} (18.2)^{\frac{1}{4}}$$

But $T_0 = \left(\frac{\lambda}{\xi^3 kN(E_f)} \right)$, where $\lambda = (18.2)$

So, $Y \approx \left(\frac{T_0}{T} \right)^{\frac{1}{4}}$ and $\Gamma = V_{ph} e^{-\left(\frac{T_0}{T} \right)^{\frac{1}{4}}}$

Then we derive the hopping conductivity:

$$\sigma = e^2 \Lambda D(0) \quad \text{where } \Lambda \text{ is the diffusion constant and } \Lambda = \Gamma r^2.$$

So,
$$\sigma = e^2 r^2 V_{ph} N(E_f) e^{-\left(\frac{T_0}{T} \right)^{\frac{1}{4}}} \quad (2.13)$$

If we assumed that $\sigma_0 = e^2 r^2 V_{ph} N(E_f)$ then the conductivity will take the form:

$$\sigma = \sigma_0 e^{-\left(\frac{T_0}{T} \right)^{\frac{1}{4}}} \quad (2.14)$$

Chapter Three

Simulation of Hopping Theory

In this chapter we evaluate the electrical conductivity in region of temperature, $100 \text{ K} \leq T \leq 300 \text{ K}$ using different light intensities (F). This chapter consists of four sections, in the first section, we divide an experimental data into three regions and find the slope and intercept for every region. In section 3.2, we find the value of density of state **DOS** at Fermi level by two methods depending on the values obtained in section 3.1. In section 3.3, we fit the values of **DOS** which are calculated in section 3.2 using *Excel M.O.*, to ensure that the value of **DOS** is constant as it is stated by the variable range hopping theory of Mott [2]. In the last section we testify a new approach for the hopping conductivity, we combine thermionic emission at all temperatures together with the hopping to show (by using simulation) if the non-constant of **DOS** is still valid or not.

3.1 Analysis of temperature regions:

To understand the idea that stands behind dividing the region of temperature into three sub-regions, we sketch the experimental data for Tl_2SSe_2 crystal under various conductivities, see Figure 1.

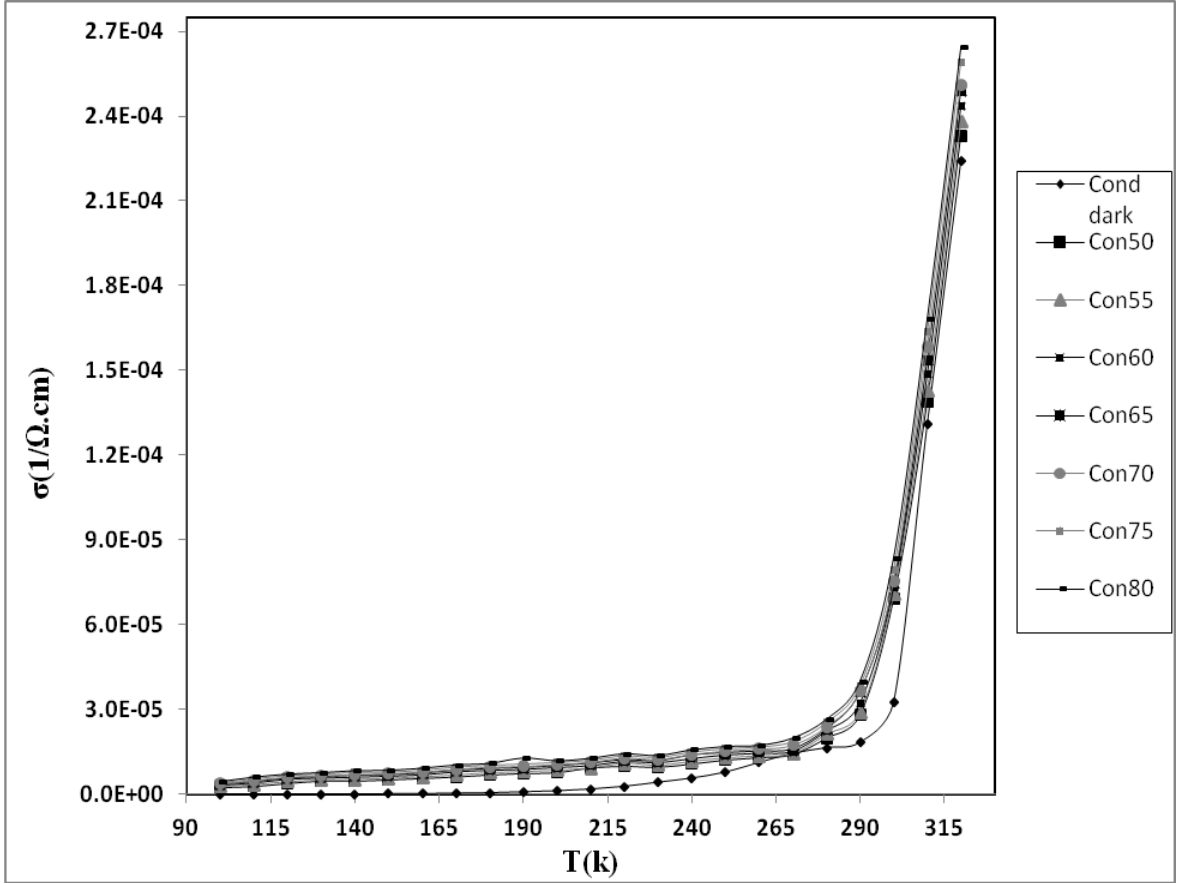


Figure 1: the conductivity with different temperature in dark and with various light intensity $F=50,55,60,65,70,75$ and 80 ($mW.cm^{-2}$), these values got from original experimental data we obtained.

From Figure 1, the conductivity variation is non-linear and exhibits exponential decay with temperature. The electrical conductivity in the dark is altered by a photon energy disturbance to check the effects of the extra photonic energy on the hopping parameters.

The plot of $\ln(\sigma) - T^{-\frac{1}{4}}$ in accordance to equation (2.14) reveals straight line with slopes and intercepts that allow determining the VRH in accordance to the equations.

For the original equation the electrical conductivity $\sigma = \sigma_2 e^{-\left(\frac{T_0}{T}\right)^{1/4}}$ obtained from Miller-Abrahams Hopping Rate with $\sigma_2 = e^2 a^2 V_{ph} N(E_F)$.

$$\text{and } R^2 = \left(\frac{9}{8 \pi \gamma k_B T N(E_F)} \right)^{\frac{1}{2}},$$

Where a and R is the average hopping range and

$$T_0 = \frac{\lambda \gamma^3}{k_B N(E_F)}, \quad N(E_F) = \frac{\lambda \gamma^3}{k_B T_0}, \quad \text{and} \quad W = \frac{3}{4\pi R^3 N(E_f)}$$

Here:

$\varepsilon = \gamma^{-1} = 5 \text{ \AA}$ is typical value.

$a = 10.78 \text{ \AA}$ is the hopping distance.

$V_{ph} = 10^{13} \text{ s}^{-1}$ is the phonon frequency.

$e = 1.6 \times 10^{-19}$ and $k_B = 86.25 \text{ meV}$.

The $\ln(\sigma) - T^{-1}$ variation can be divided into two regions :

a) The range of high temperature, which is between 270 k and 320 k. In this region

we consider the equation $\sigma = \sigma_0 e^{-\left(\frac{E_a}{KT}\right)}$, this equation is selected because it represent the pure thermionic emission of charged carriers over the energy barriers

that exist in the material. Thermionic emission in dominate at very high temperature. The natural logarithm of both sides yields the equation

$\ln \sigma = -\left(\frac{Ea}{KT}\right) + \ln \sigma_0$. Then we plot $\ln(\sigma)$ versus $1000/T$ of the experimental data

with different values of light intensity. So, graphically the values of $\frac{Ea}{1000K}$ and

$\ln \sigma_0$ are the slope and y-intercept respectively, see Table 1 and Figure 2.

Table 1: values of E_a and σ_0 get from the plot of experimental data of Conductions with different temperature along the range T(320-270)K indicative for a variable light intensity F ($mW.cm^{-2}$).

320-270 K				
F ($mW.cm^{-2}$)	slope	Intercept	E_a (eV)	σ_0 ($\Omega.cm^{-1}$)
Dark	5.0488	7.3219	0.435	1.51E+03
50	5.0092	7.2256	0.432	1.37E+03
55	4.9821	7.1664	0.430	1.30E+03
60	4.9389	7.0569	0.426	1.16E+03
65	4.8912	6.9287	0.422	1.02E+03
70	4.7842	6.6011	0.413	7.36E+02
75	4.7289	6.459	0.408	6.38E+02
80	4.6626	6.2757	0.402	5.31E+02

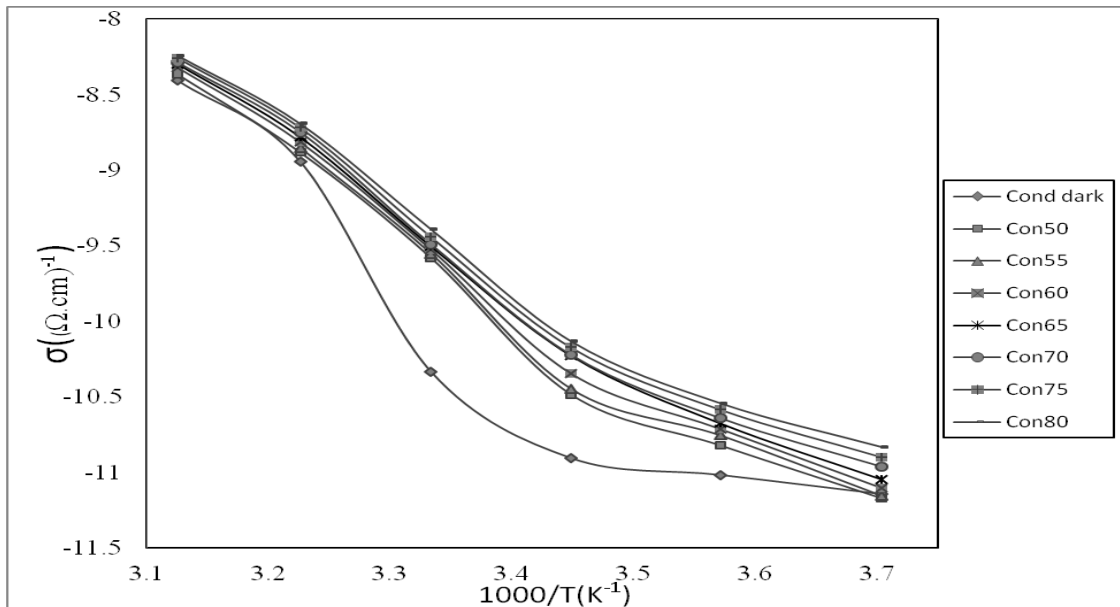


Figure 2: the Conduction with different temperature along the range T(320-270)K, showing a $\ln\sigma \sim 1/(1000/T)$ dependence, indicative for a variable light intensity $F = 50, 55, 60, 65, 70, 75$ and 80 ($mW.cm^{-2}$).

As it is easily observed from the figure, no linear region is observed.

b) The middle range of temperature which is between 140 k and 260 k. In this region

we consider the equation $\sigma = \sigma_2 e^{-\left(\frac{T_0}{T}\right)^{\frac{1}{4}}}$ (Mott's variable range hopping), which

is for the conductivity at low temperature. We use the experimental data at the

specified range to draw the relation $\ln(\sigma) = -\left(\frac{T_0}{T}\right)^{\frac{1}{4}} + \ln \sigma_2$. Figure 3-a shows

the best linear curve that fit the experimental data in dark and Figure 3-b shows the

linear curves at $F = 50, 55, 60, 65, 70, 75$ and $80 (mW.cm^{-2})$. From the graphs we find

the values of $\ln \sigma$ and $\left(\frac{1}{T}\right)^{\frac{1}{4}}$ which are the slope and y-intercept see table 2.

Table 2: values of T_0 and σ_2 get from the plot of experimental data of Conductions with different tempreture along the range T(260-140)K indicative for a variable light intensity $F (mW.cm^{-2})$.

260-140				
$F (mW.cm^{-2})$	Slope	Intercept	$T_0 (K)$	$\sigma_2 (\Omega cm)^{-1}$
Dark	120.63	18.552	2.12E+08	1.14E+08
50	24.35	-5.2255	3.52E+05	5.38E-03
55	23.015	-5.4986	2.81E+05	4.09E-03
60	21.582	-5.8023	2.17E+05	3.02E-03
65	20.861	-5.9204	1.89E+05	2.68E-03
70	20.172	-6.0471	1.66E+05	2.36E-03
75	19.291	-6.2262	1.38E+05	1.98E-03
80	18.461	-6.3944	1.16E+05	1.67E-03

The table shows a sharp drop in the value of the disorder degree from 10^8 K in the dark to 10^5 under light excitation. This strange drop is of importance because it means reduction of electronic disordering by three orders of magnitude. It in turn lead to improvement of the performance of RAM device through very cheap led lightening by three orders.

In according to VRH theory T_0 must remain constant as it depends on DOS of material that is established during the device design. However, the photon excitations reduced these values sufficiently. The value of T_0 clarifies the problem; we compute the other physical parameters to observe the side effects.

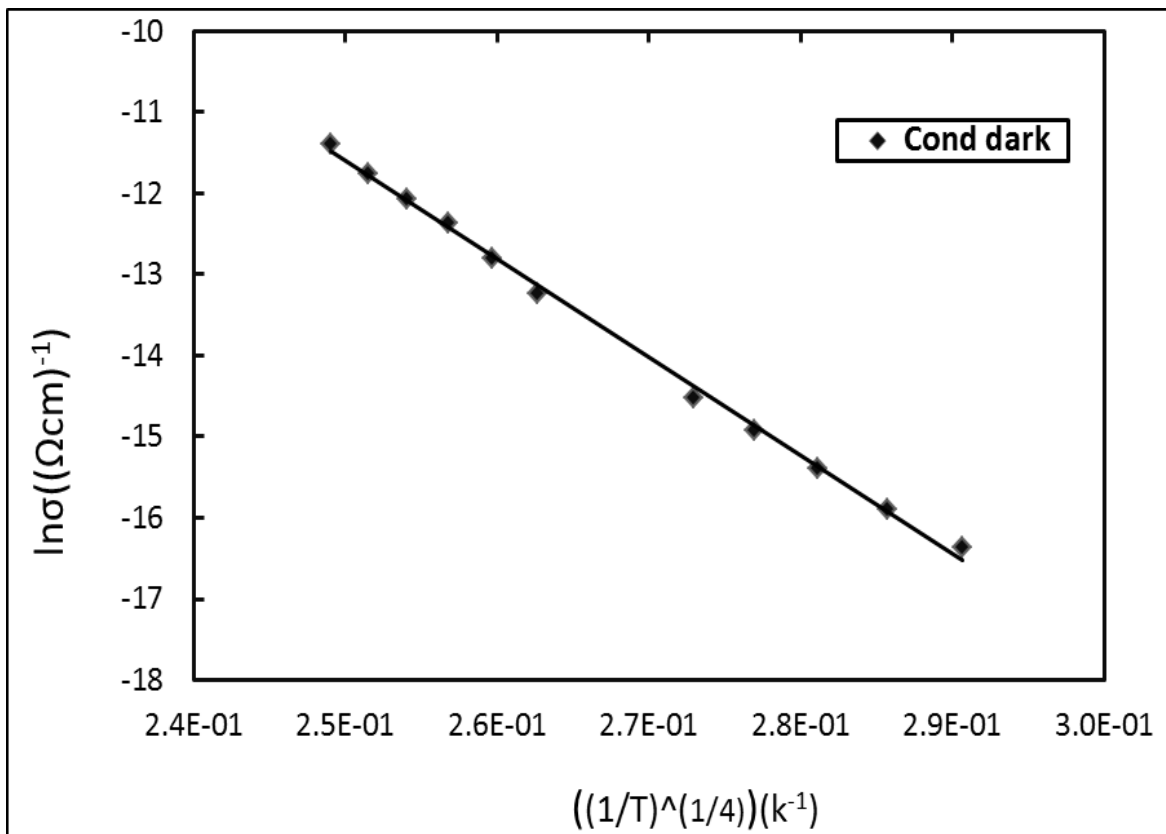


Figure 3- a : Conduction with different temperature along the range T(260-140)K, showing $\ln\sigma \sim (T)^{-1/4}$ dependence, with no light intensity (dark).

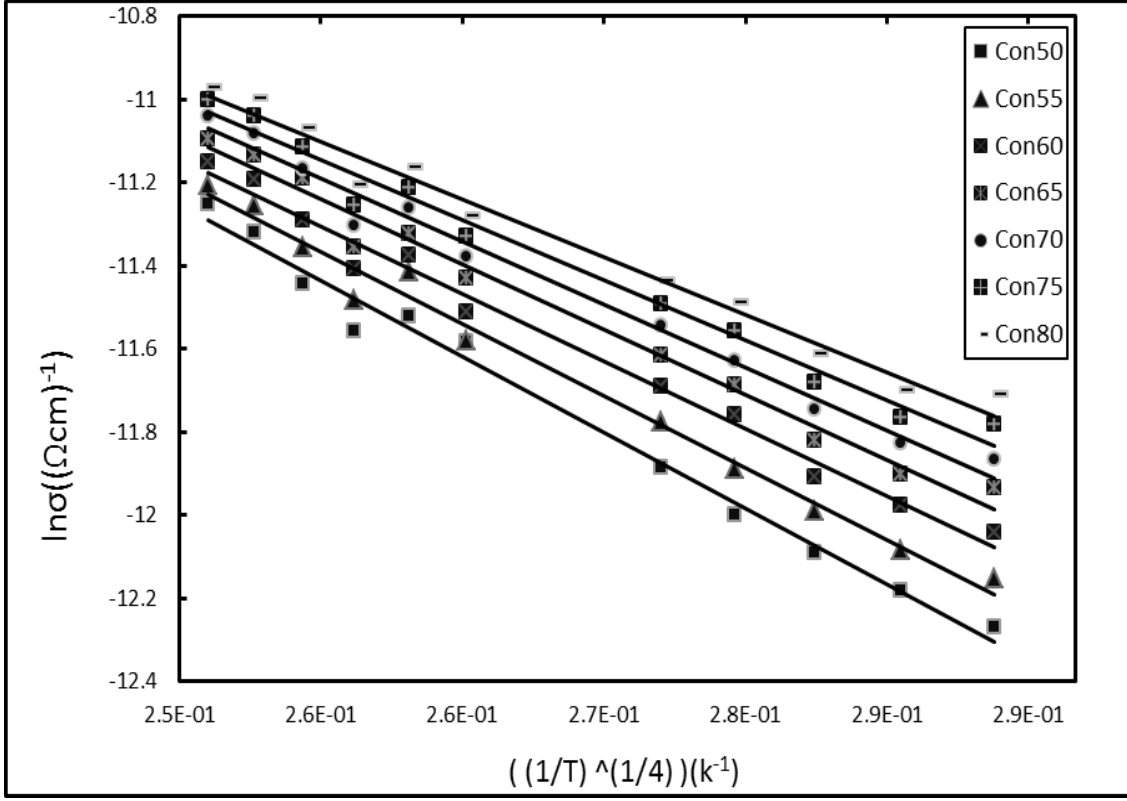


Figure 3- b: Conduction with different temperature along the range $T(260-140)K$, showing a $\ln\sigma \sim (T)^{\frac{1}{4}}$ dependence, indicative for a variable light intensity $F = 50, 55, 60, 65, 70, 75$ and $80 (mW.cm^{-2})$.

3.2 Computation of the density of state at Fermi level

In this section we use the computed values of the conductivity parameters in section 3.1 to compute the value of $N(E_f)$. In fact, there are two methods for that, in the first method assuming the percolation constant $\lambda = 18.1$ and the density of state at Fermi level is given by the equation: $N(E_F) = \frac{\lambda \gamma^3}{k_B T_0}$. So, we use the values $(T_0)^{\frac{1}{4}}$,

and $\gamma = \xi^{-1} = (5^\circ A)^{-1} = 2 \times 10^9$. Then,

$$N(E_F) = \frac{18.1 \times (2 \times 10^9)^3}{86.25 \times T_0} = 1.67884058 \times 10^{27} \times \left(\frac{1}{T_0}\right) \quad (3.1-a)$$

and the values of R and W are as follows:

$$R = \left(\frac{9}{8 \times 3.14 \times 2 \times 10^9 \times 86.25 \times 150 \times N(E_F)} \right)^{1/4} = 3.4303278 \times 10^{-4} \times \left(\frac{1}{N(E_F)} \right)^{1/4} \quad (3.1-b)$$

$$W = \left(\frac{3}{4 \times 3.14 \times R^3 \times N(E_F)} \right) = \frac{3}{4 \times 3.14 \times R^3 \times N(E_F)} = 0.238853503 \times \frac{1}{R^3 N(E_F)} \quad (3.1-c)$$

In the second method we get use from the pre-exponential factor presented by the equation:

$$\sigma_2 = e^2 a^2 v_{ph} N(E_F)$$

Here the percolation constant λ may be a reason for the variation of DOS under light and thus it is assumed to be a rather than constant function.

$$a^2 = R^2 = \left(\frac{9}{8 \pi \gamma k_B T N(E_F)} \right)^{1/2}. \text{ On the other hand, since } T_0 = \frac{\lambda \gamma^3}{k_B N(E_F)} \text{ we have}$$

$$\gamma = \left(\frac{T_0 k_B N(E_F)}{\lambda} \right)^{1/3}. \text{ Then } \sigma_2 = e^2 \left(\frac{9 N(E_F)}{8 \pi \gamma k_B T} \right)^{1/2} v_{ph}.$$

Thus;

$$\frac{\sigma_2}{e^2 v_{ph}} = \left(\frac{9 N(E_F)}{8 \pi \left(\frac{T_0 k_B N(E_F)}{\lambda} \right)^{1/3} k_B T} \right)^{1/2} = \left(\frac{9}{8 \pi T} \left(\frac{\lambda}{T_0 k_B^4} \right)^{1/3} \right)^{1/2} N(E_F)^{1/3}.$$

$$\text{So, } N(E_F) = \left(\frac{\sigma_2}{e^2 v_{ph}} \right)^3 \left(\frac{8 \pi T}{9} \left(\frac{T_0 k_B^4}{\lambda} \right)^{1/3} \right)^{3/2} = \left(\frac{8 \pi T k_B^{4/3}}{9 e^4 v_{ph}^2} \right)^{3/2} (\sigma_2)^3 \left(\frac{T_0}{\lambda} \right)^{1/2}$$

$$N(E_F) \text{ at } T = 150 = \left(\frac{8 \times 3.14 \times 150 \times (86.25)^{4/3}}{9 \times (1.6 \times 10^{-19})^4 \times 10^{26}} \right)^{3/2} (\sigma_2)^3 \left(\frac{T_0}{\lambda} \right)^{1/2}$$

$$N(E_F) = 3.798401673 \times 10^{81} (\sigma_2)^3 \left(\frac{T_0}{\lambda} \right)^{1/2} \quad (3.2)$$

$$\gamma = \left(\frac{T_0 K_B N(E_f)}{\lambda} \right)^{1/3} = \left(\frac{(86.25) T_0 N(E_f)}{\lambda} \right)^{1/3},$$

Now we try to evaluate the value of λ using Fitting Curve method in Excel, for more details see Appendix A. From the excel work sheet we can find the value of λ , see the Table 3 below.

Table3: actual and predicted values of $N(E_f)$ using the two methods.

Method#1: from T_0 and y			Method#2 from T_0 and σ_2				
$N(E_f)$	R	W	$N(E_f)$ predict	R	W	$N(E_f)$ pred- $N(E_f)$	diff ²
7.93E+18	1.92E+01	4.23E-24	2.41E+56	4.52E+10	1.07E-89	2.41E+56	5.82E+112
4.78E+21	9.53E+01	5.77E-29	1.03E+24	365.4659	4.75E-33	1.03E+24	1.05E+48
5.98E+21	1.01E+02	3.89E-29	4.06E+23	289.4999	2.43E-32	4.00E+23	1.60E+47
7.74E+21	1.08E+02	2.48E-29	1.43E+23	223.2376	1.5E-31	1.36E+23	1.84E+46
8.86E+21	1.11E+02	1.95E-29	9.41E+22	200.873	3.13E-31	8.52E+22	7.26E+45
1.01E+22	1.15E+02	1.54E-29	6.01E+22	179.622	6.85E-31	5.00E+22	2.50E+45
1.21E+22	1.20E+02	1.13E-29	3.21E+22	153.5769	2.05E-30	2.00E+22	4.01E+44
1.45E+22	1.26E+02	8.31E-30	1.78E+22	132.4311	5.79E-30	3.32E+21	1.10E+43
	λ	5.91E+106				sum of diff ²	5.82E+112

The solution reveals an infinite value of λ . This type of solution finds no correct result. A well apparent conflict between the experimentally observed and the computed is better shown in Figure 4. $N(E_F)$ Increases with F, but the theoretical one decreases with F.

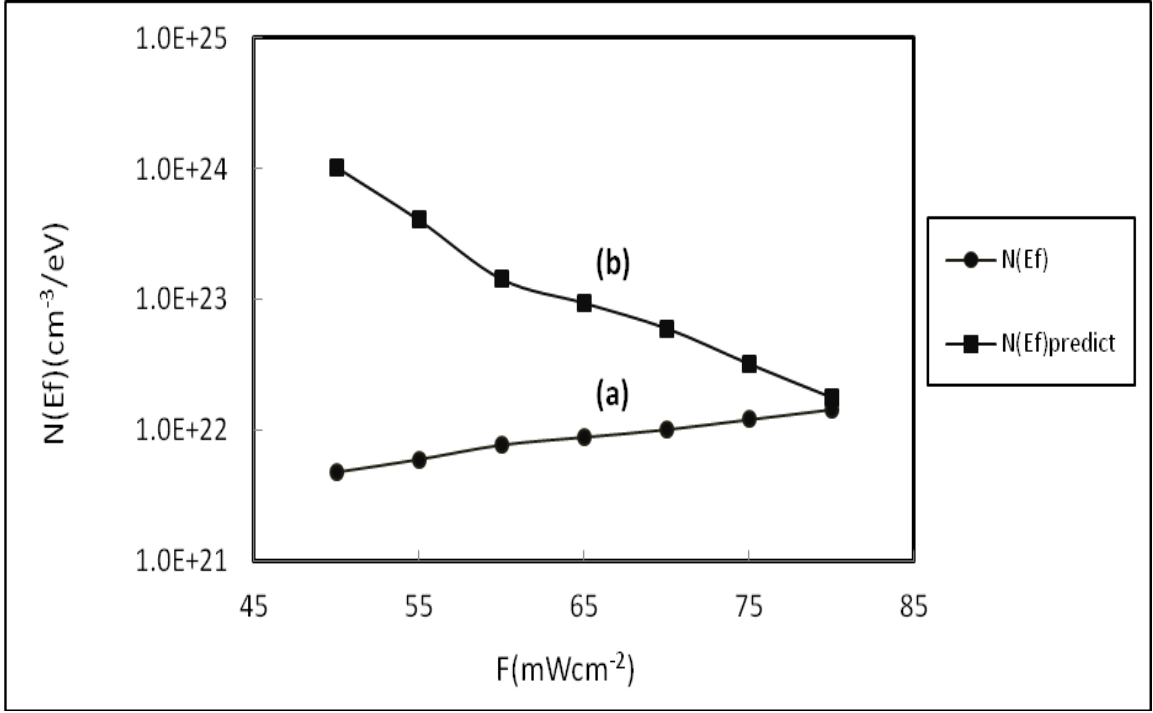


Figure 4: $N(E_f)$ with different intensity light, showing (a) actual points and (b) the predicted values at some value of $\lambda=5.91E+106=$ infinity.

Thus when we have λ as a variable with F and since the DOS is a variable of λ , the DOS is not constant but variable of F . Now we will find λ for all points (for all F) by: fitting the values of actual $N(E_F)$ get from equation (3.1.a) with the values of predicted $N(E_F)$ get from equation (3.2), and we do that as following:

$$N(E_F) = N(E_F)_{predicted}$$

$$\frac{18.1 \times (2 \times 10^9)^3}{86.25 \times T_0} = 1.67884058 \times 10^{27} \times \left(\frac{1}{T_0}\right) = 3.798401673 \times 10^{81} (\sigma_2)^3 \left(\frac{T_0}{\lambda}\right)^{1/2} \quad (3.3)$$

In equation (3.3) there is only one unknown parameter, which is λ , see Table 4.

Table 4: values of λ for different light intensity get from fitting.

$\lambda^{1/2}$	λ
3.29E-38	1.08E-75
4.63E-03	2.15E-05
1.47E-02	2.17E-04
5.39E-02	2.91E-03
9.42E-02	8.88E-03
1.69E-01	2.84E-02
3.77E-01	1.42E-01
8.13E-01	6.62E-01

In the scope of this analysis, it turn out that γ cannot be constant but a variable that depends on F . Table 5; show the computed γ -values in the scope of these assumptions. The γ value is much less than one atomic orbit radius. The minimum allowed value of electron in H-atom is $5.11 \times 10^{-11} m$. So the calculated length being $10^{-35}, 10^{-12}$ is impossible.

Now, we can find γ by use the values of λ (in Table 4), T_0 and actual values of $N(E_F)$ and then find $\xi = 1/\gamma$, $\gamma R = \gamma \times R$, (see Table 5). We find all of that to prove the validity of DOS when it is not constant.

Table5: values of γ , $(1/\gamma)$ and γR get from the values of λ .

$\gamma (cm^{-1})$	$\xi (cm)$	γR
5.12E+34	1.95E-35	9.85E+35
1.89E+11	5.29E-12	1.80E+13
8.73E+10	1.15E-11	8.81E+12
3.68E+10	2.72E-11	3.96E+12
2.54E+10	3.94E-11	2.82E+12
1.72E+10	5.81E-11	1.98E+12
1.01E+10	9.94E-11	1.21E+12
6.03E+09	1.66E-10	7.58E+11

3.3 Approach of Mixed conduction

In this section we try another approach and we assume the existence of mixed conduction and the mixture is composed of thermionic emission at all temperatures and hopping.

This approach is considered because the high region of temp did not show linear variation with reciprocal temperature.

We look at the relation $\ln \sigma = \ln \sigma_0 - \frac{E}{kT}$ as a function of $(kT)^{-1}$ then the differential activation energy is given by the relation $dE_a = \frac{-d(\ln(\sigma))}{d(kT)^{-1}}$. The values of dE_a at various values of light intensity are to be calculated. We draw the graph of dE_a versus the temperature (T) on the same diagram to see the efficiency of the use of thermionic

emission conductivity on the range of temperature (140-320) K, the results are displayed in Figure 5.

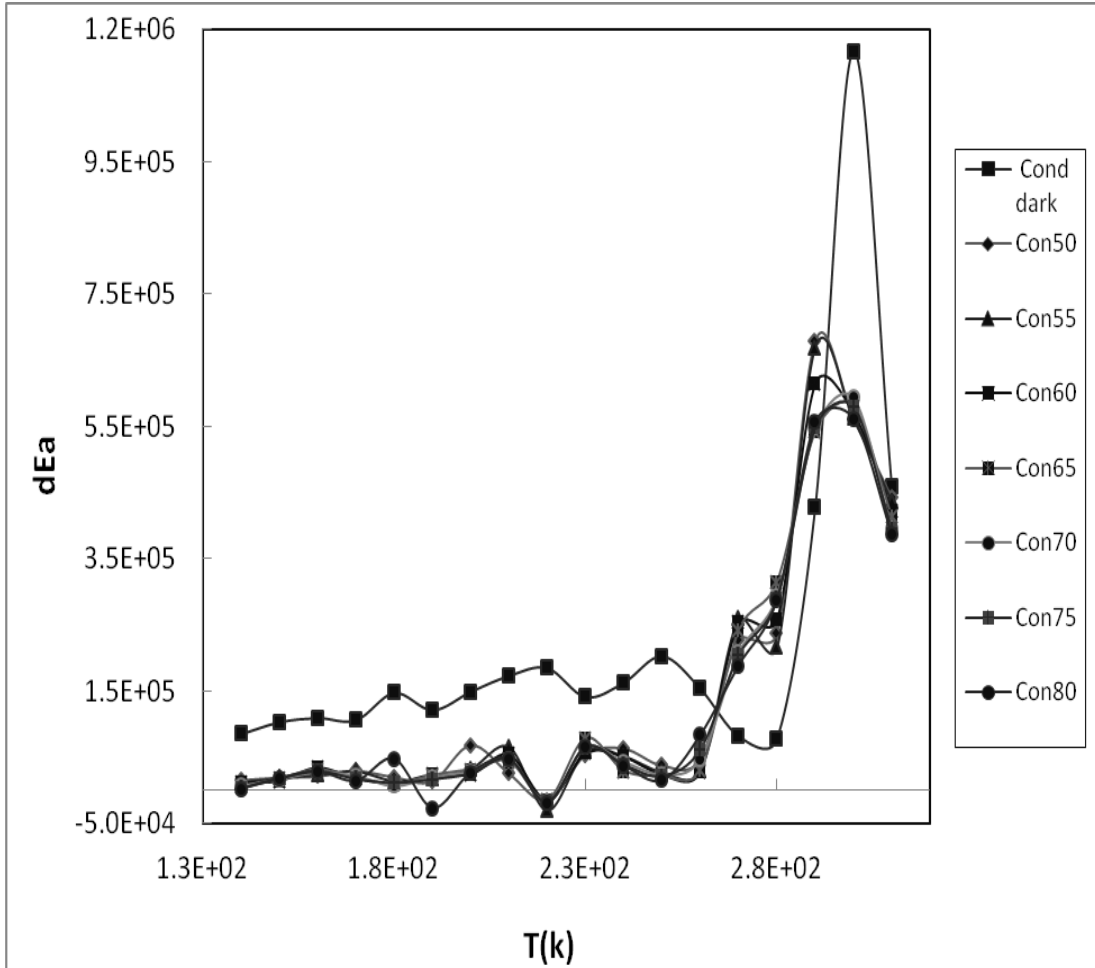


Figure 5: dE_a with different temperature along the range T (320-140) K, showing non-linear relation between dE_a (derivative of E_a) and the temperature, indicative for a variable light intensity at values $F = 50-80 (mW.cm^{-2})$.

As Figure 5, show the relationship between dE_a and the temperature (T) is nonlinear. This lead us to assume that the mechanism is the mixed conduction. According to this assumption we try to find values for T_0 and E_a which are valid for any temperature as well as any light intensity F . For that object we draw the graph of

the conduction, which is obtained experimentally together with the mixed conduction.

The details of this approach are considered by using σ_0 and σ_2 from experiment as:

$$\sigma(T) = \sigma_0 e^{-\left(\frac{E_a}{kT}\right)} + \sigma_2 e^{-\left(\frac{T_0}{T}\right)^{1/4}}$$

See appendix B (Figures B1-B7).

Using this approach the evaluated E_a and T_0 are displayed in Table 1 (see Table 6).

Table 6: values of E_a and T_0 we get from the fitting plots in Figures B(1-8) (in appendix B) at different light intensity.

$F (mW.cm^{-2})$	$E_a (eV)$	$T_0 (k)$
Dark	4.41E-01	2.08E+08
50	4.06E-01	3.45E+05
55	4.61E-01	2.74E+05
60	4.38E-01	2.12E+05
65	4.10E-01	1.83E+05
70	4.39E-01	1.61E+05
75	4.43E-01	1.33E+05
80	4.10E-01	1.12E+05

Although the E_a variation did not show systematic change with light intensity, the values of the degree of disorder systematical fall down. This determent is best shown in Figure 6.

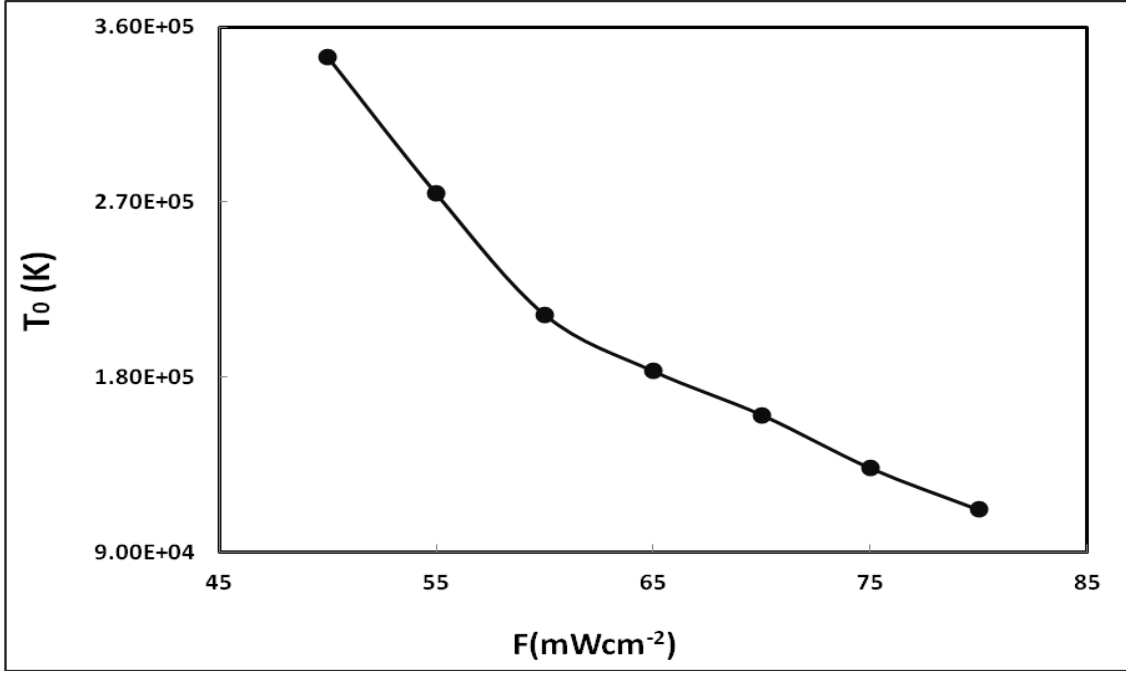


Figure 6 : T_0 (get from fitting) with different light intensity F ($mW.cm^{-2}$).

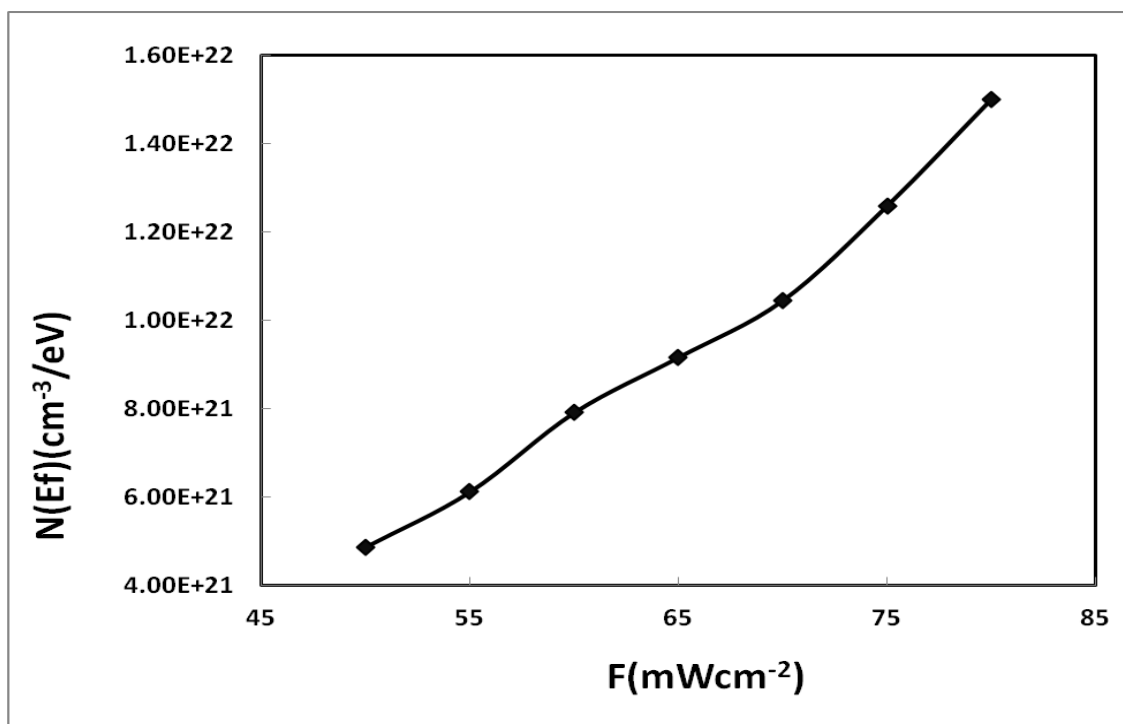
From the values of T_0 , the peremeters $N(E_F)$, R , W , γ and γR can be founded.

$$N(E_F) \text{ By Equation (3.1-a): } \quad N(E_F) = 1.67884058 \times 10^{27} \times \left(\frac{1}{T_0}\right) .$$

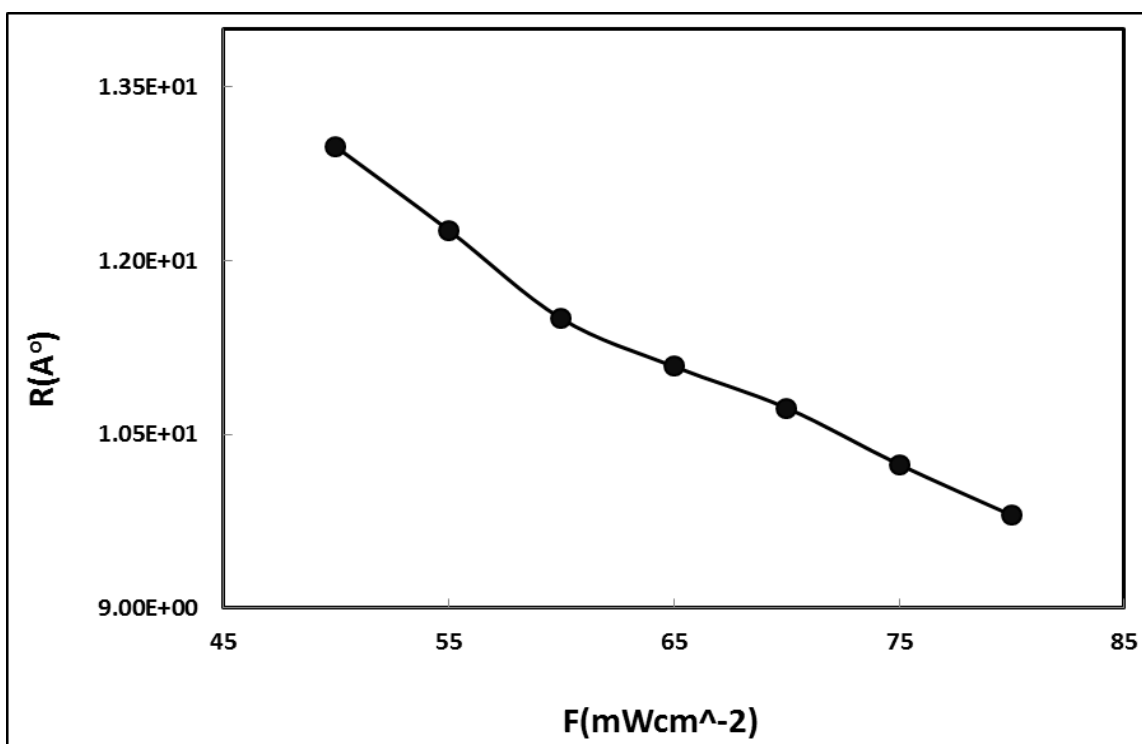
$$\text{And } R \text{ by Equation (3.1-b): } \quad R = 3.4303278 \times 10^{-4} \times \left(\frac{1}{N(E_F)}\right)^{1/4} .$$

$$\text{We find } W \text{ by Equation (3.1-c): } \quad W = 0.238853503 \times \frac{1}{R^3 N(E_F)} .$$

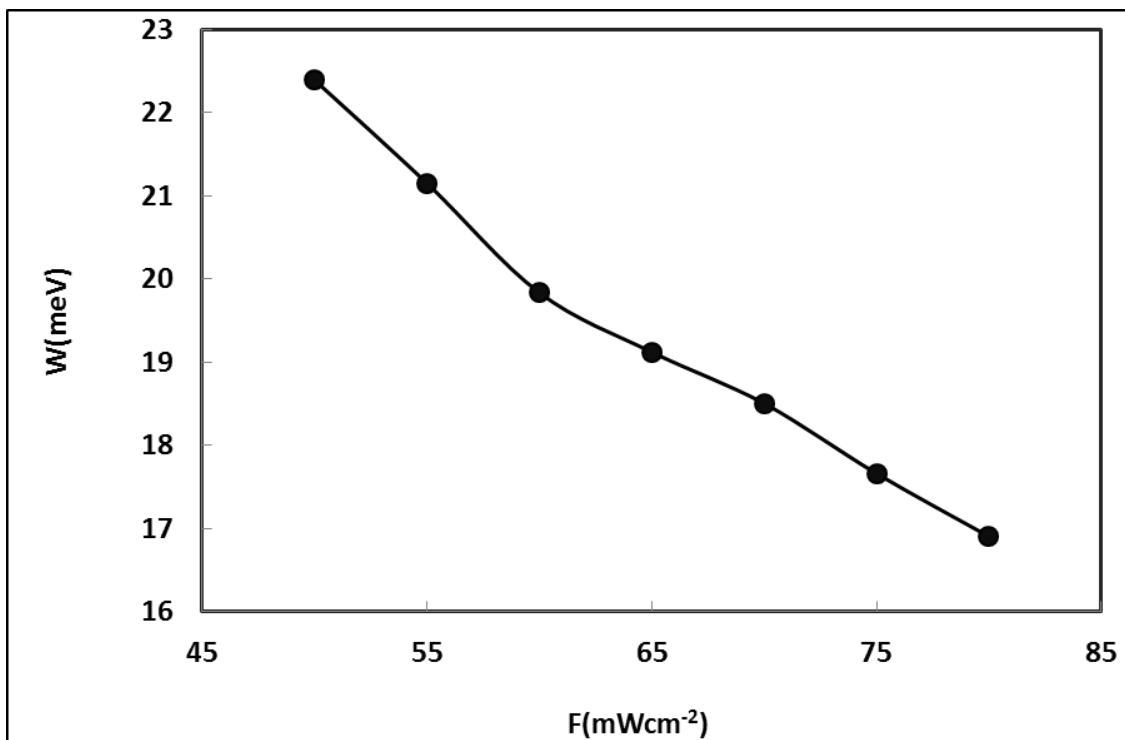
From Tables 6 which gives the values of T_0 and equations 3.1(a-c) together with the equation $\gamma R = 2 \times 10^9 \times R$ we can calculate the peremeters $N(E_F)$, R , W , γ and γR as follows, see Figures 7(a-d).



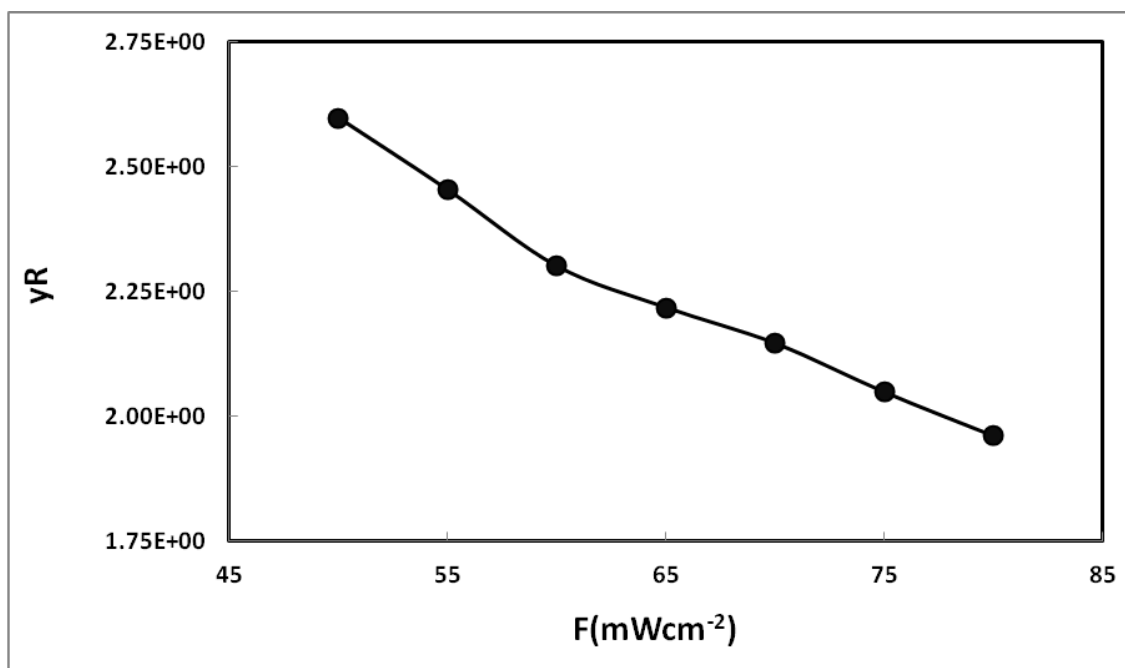
Figures7 a: $N(E_f)$ with different light intensity $F (mW.cm^{-2})$.



Figures7 b: R with different light intensity $F (mW.cm^{-2})$.



Figures7 c: W with different light intensity F ($mW.cm^{-2}$).



Figures7 d: γR with different light intensity F ($mW.cm^{-2}$).

The data displayed in Figure 6 are consistent with our obtained experimental data. This approach may be regarded as correct solution. However, the correcting of the Mott's variable range hopping theory is questionable.

Chapter four

Result and Discussion (non-constant DOS):

In this chapter we compute the hopping conductivity for non-constant density of state (DOS) which we proved it is validity in previous chapter. This chapter consists of two sections, in section one, we give a full mathematical analysis to the model of S.Boutiche [44] for the non-constant DOS (**polynomial**) and Mott principles for the constant DOS, and in section two, we discuss numerically the model of the **exponential** density of state (DOS) and the model of Mott principles for the constant DOS.

4.1 The polynomial DOS:

According to the variable range hopping theory of Mott [2], $N(E_f)$ is assumed as an energy-independent distribution, and a large number of previous studies on carrier transport [40-43], in particular in amorphous, micro (or nano) crystalline silicon layers, reported the average value of the material. Also by the variable range hopping theory of Mott [2], the temperature T dependence of the conductivity, when conduction between localized states near Fermi level E_f is by hopping, is given by equation (1.1). And we talked about the derivation of equation (1.1), in chapter two. Mott has minimized the argument of the following equation:

$$\sigma_{ij} = \exp \left\{ -2\alpha R_{ij} - \frac{E_{ij}}{kT} \right\} \quad (4.1)$$

With respect to the distance hop R_{ij} , he assumed that the density of states is constant over the energy range of hopping:

$$N(E) = N(E_F) \approx \left(\frac{1}{E_{ij} R_{ij}^3} \right) \quad (4.2)$$

Is constant as the hopping energy ranges between 0.1–0.2 eV . It is hard to believe that $N(E)$ remains constant over such energy range. But what equations (1.1) and (4.2) becomes if the density of states is non-constant near E_F ?

S. Boutiche [44], discussed numerically the hopping conductivity for polynomial density of states (**DOS**) using percolation theory. Boutiche add some assumptions about the shape of $N(E)$, first he consider that $N(E_F)$ is the density of states at Fermi level, and he suppose that the asymmetric part of $N(E)$ follows an odd power law form. So,

$$\begin{aligned} N(E) &= N(E_F) + s_q E^q \\ N(E) &= N(E_F) [1 + v_q E^q] \end{aligned} \quad (4.3)$$

Where $q = 1, 3, 5 \dots$, and s_q is a positive constant (s_q is the slope for the linear case of $N(E)$), the energy E is measured from the Fermi level $E_F = 0$.

There are two critical conditions must be satisfied: the first concerns the nature of each conductance σ_{ij} given equation (4.1). In fact, each conductive must be at least equal to the critical conductivity σ_c :

$$\sigma_{ij} \geq \sigma_c \quad (4.4)$$

And the second condition concerns the average number $\langle m(E_i) \rangle$ of conductance linked to each site located at energy E_i . Such a number must be equal at least to a critical concentration “c” of links per site:

$$c = \langle m(E_i) \rangle \quad (4.5)$$

When the conditions (4.4) and (4.5) are satisfied it appears in the random network a critical path of conductances joining one side of the system to the other. The problem of the random network is said solved only when σ_c is correctly identified and this happens when equation (4.5) is solved [44].

Resolution of the random network problem of conductances by Boutiche:

Boutiche used equation (4.1) to rewrite equation (4.4) under the form:

$$\exp\left\{-2\alpha R_{ij} - \frac{E_{ij}}{kT}\right\} \geq \exp\left\{-\frac{E_m}{kT}\right\} \quad (4.6)$$

Where E_m is the energy at critical conductivity (highest energy) in the center of the sphere with radius $R = 0$, and it must be identified to solve our random network problem. Boutiche used equation (4.3) to evaluate the number $m(E_i)$, it is necessary to count all sites located at energies E_j accessible by the electron located at the site of energy E_i . Such E_j sites are randomly distributed within a sphere of radius R_{ij} and from equation (4.6), R_{ij} satisfy the relation:

$$R_{ij} \leq \frac{1}{2\alpha kT} (E_m - E_{ij}) \quad (4.7)$$

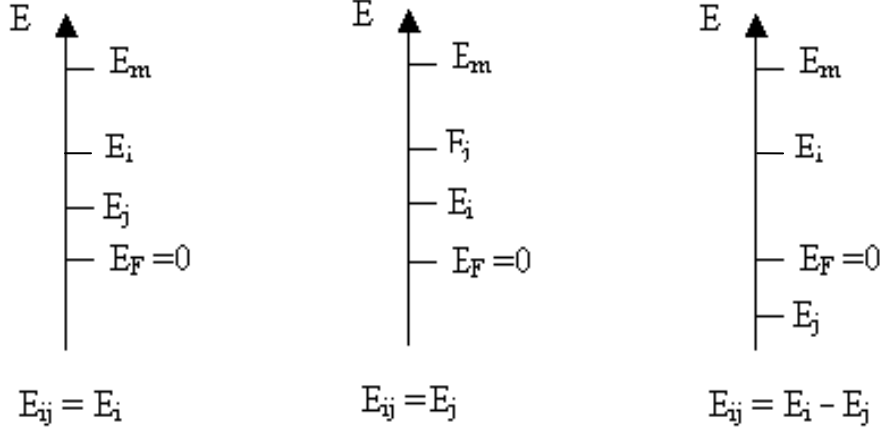
On the other hand, $m(E_i)$ is given by the formula:

$$m(E_i) = \frac{4\pi}{3} \int R_{ij}^3 N(E_j) dE_j \quad (4.8)$$

From relation (4.7) and equation (4.8) we obtain:

$$m(E_i) = \frac{4\pi}{3} \frac{1}{(2\alpha kT)^3} \int (E_m - E_{ij})^3 N(E_j) dE_j \quad (4.9)$$

Without loss of generality we may assume that $E_i > 0$. So, if we integrate overall E_{ij} then E_j has the following possible situations besides the possible values for E_{ij} .



Limits: $0 \longrightarrow E_i$ $E_i \longrightarrow E_m$ $-(E_m - E_i) \longrightarrow 0$

On the other hand, the limits of the integral are the boundaries of the smallest interval which contains E_j . Hence the corresponding intervals are $[0, E_i]$, $[E_i, E_m]$ and $[-(E_m - E_i), 0]$. Therefore from equations (4.3) and (4.9), we have

$$m(E_i) = \frac{4\pi}{3} \frac{N(E_F)}{(2\alpha kT)^3} \left\{ \int_0^{E_i} (E_m - E_i)^3 (1 + \nu_q E_j^q) dE_j + \int_{E_i}^{E_m} (E_m - E_j)^3 (1 + \nu_q E_j^q) dE_j + \int_{-(E_m - E_i)}^0 (E_m - E_i + E_j)^3 (1 + \nu_q E_j^q) dE_j \right\}$$

We let: $I_1 = \int_0^{E_i} (E_m - E_i)^3 (1 + \nu_q E_j^q) dE_j$, $I_2 = \int_{E_i}^{E_m} (E_m - E_j)^3 (1 + \nu_q E_j^q) dE_j$ and

$$I_3 = \int_{(E_i - E_m)}^0 (E_m - E_i + E_j)^3 (1 + \nu_q E_j^q) dE_j = \int_{(E_i - E_m)}^0 (E_j - (E_i - E_m))^3 (1 + \nu_q E_j^q) dE_j,$$

$$\text{Then } m(E_i) = \frac{4\pi}{3} \frac{N(E_F)}{(2\alpha kT)^3} (I_1 + I_2 + I_3) \quad , \quad (4.10)$$

The first integral,

$$I_1 = E_i (E_m - E_i)^3 \left[1 + \frac{v_q}{q+1} E_i^q \right] = E_m^4 x(1-x)^3 + \frac{v_q}{q+1} E_m^{q+4} x^{q+1} (1-x)^3 \quad (4.11)$$

Where $x = \frac{E_i}{E_m}$. We note here that $E_i > 0$.

The second integral can be simplified as follows:

$$I_2 = \int_{E_i}^{E_m} (E_m^3 - 3E_m^2 E_j + 3E_m E_j^2 - E_j^3) dE_j + v_q \int_{E_i}^{E_m} (E_m^3 E_j^q - 3E_m^2 E_j^{q+1} + 3E_m E_j^{q+2} - E_j^{q+3}) dE_j$$

Hence

$$\begin{aligned} I_2 &= \left[E_m^3 E_j - \frac{3}{2} E_m^2 E_j^2 + E_m E_j^3 - \frac{E_j^4}{4} \right]_{E_i}^{E_m} + v_q \left[\frac{E_m^3 E_j^{q+1}}{q+1} - \frac{3}{q+2} E_m^2 E_j^{q+2} + \frac{3}{q+3} E_m E_j^{q+3} - \frac{E_j^{q+4}}{q+4} \right]_{E_i}^{E_m} \\ I_2 &= (E_m^4 - \frac{3}{2} E_m^4 + E_m^4 - \frac{E_m^4}{4}) - (E_m^3 E_i - \frac{3}{2} E_m^2 E_i^2 + E_m E_i^3 - \frac{E_i^4}{4}) \\ &+ v_q \left(\frac{E_m^{q+4}}{q+1} - \frac{3}{q+2} E_m^{q+4} + \frac{3}{q+3} E_m^{q+4} - \frac{E_m^{q+4}}{q+4} \right) - v_q \left(\frac{E_m^3 E_i^{q+1}}{q+1} - \frac{3}{q+2} E_m^2 E_i^{q+2} + \frac{3}{q+3} E_m E_i^{q+3} - \frac{E_i^{q+4}}{q+4} \right) \\ I_2 &= \frac{E_m^4}{4} + v_q E_m^{q+4} \left(\frac{1}{q+1} - \frac{3}{q+2} + \frac{3}{q+3} - \frac{1}{q+4} \right) - E_m^4 \left(x - \frac{3x^2}{2} + x^3 - \frac{x^4}{4} \right) - v_q E_m^{q+4} \left(\frac{x^{q+1}}{q+1} - \frac{3x^{q+2}}{q+2} + \frac{3x^{q+3}}{q+3} - \frac{x^{q+4}}{q+4} \right) \end{aligned}$$

So,

$$I_2 = \frac{E_m^4}{4} + v_q E_m^{q+4} \left[\frac{6q!}{(q+4)!} \right] - E_m^4 \left(x - \frac{3x^2}{2} + x^3 - \frac{x^4}{4} \right) - v_q E_m^{q+4} \left(\frac{x^{q+1}}{q+1} - \frac{3x^{q+2}}{q+2} + \frac{3x^{q+3}}{q+3} - \frac{x^{q+4}}{q+4} \right) \quad (4.12)$$

The third integral also can be simplified in the following way

$$\begin{aligned} I_3 &= \int_{(E_i - E_m)}^0 (E_j^3 - 3E_j^2 (E_i - E_m) + 3E_j (E_i - E_m)^2 - (E_i - E_m)^3) dE_j \\ &+ v_q \int_{(E_i - E_m)}^0 (E_j^{q+3} - 3E_j^{q+2} (E_i - E_m) + 3E_j^{q+1} (E_i - E_m)^2 - E_j^q (E_i - E_m)^3) dE_j \end{aligned}$$

Thus,

$$I_3 = \left[\frac{E_j^4}{4} - E_j^3(E_i - E_m) + \frac{3}{2}E_j^2(E_i - E_m)^2 - E_j(E_i - E_m)^3 \right]_{(E_i - E_m)}^0$$

$$+ v_q \left[\frac{E_j^{q+4}}{q+4} - \frac{3}{q+3}E_j^{q+3}(E_i - E_m) + \frac{3}{q+2}E_j^{q+2}(E_i - E_m)^2 - \frac{E_j^{q+1}}{q+1}(E_i - E_m)^3 \right]_{(E_i - E_m)}^0$$

$$I_3 = - \left[\frac{(E_i - E_m)^4}{4} - (E_i - E_m)^4 + \frac{3}{2}(E_i - E_m)^4 - (E_i - E_m)^4 \right]$$

$$- v_q \left[\frac{(E_i - E_m)^{q+4}}{q+4} - \frac{3}{q+3}(E_i - E_m)^{q+4} + \frac{3}{q+2}(E_i - E_m)^{q+4} - \frac{(E_i - E_m)^{q+4}}{q+1} \right]$$

$$\text{So, } I_3 = \frac{E_m^4(1-x)^4}{4} - v_q E_m^{q+4}(1-x)^{q+4} \left[\frac{6q!}{(q+4)!} \right] \quad (4.13)$$

From equations (4.11- 4.13) we have:

$$I_1 + I_2 + I_3 = E_m^4 \left[x(1-x)^3 + \frac{1}{4} - \left(x - \frac{3x^2}{2} + x^3 - \frac{x^4}{4} \right) + \frac{(1-x)^4}{4} \right]$$

$$+ v_q E_m^{q+4} \left[\left[\frac{x^{q+1}(1-x)^3}{q+1} - \left(\frac{x^{q+1}}{q+1} - \frac{3x^{q+2}}{q+2} + \frac{3x^{q+3}}{q+3} - \frac{x^{q+4}}{q+4} \right) \right] + \frac{6q!}{(q+4)!} \left[1 - (1-x)^{q+4} \right] \right]$$

$$I_1 + I_2 + I_3 = \frac{E_m^4}{2} (1+x)(1-x)^3 + v_q E_m^{q+4} \left\{ \frac{6q!}{(q+4)!} (1 - (1-x)^{q+4}) - \frac{3}{q+1} \left(\frac{x^{q+2}}{q+2} - \frac{2x^{q+3}}{q+3} + \frac{x^{q+4}}{q+4} \right) \right\}$$

Therefore,

$$m(\text{Ei}) = \frac{4\pi}{3} \frac{N(\text{E}_F)}{(2\alpha kT)^3} \left\langle \frac{E_m^4}{2} (1+x)(1-x)^3 + v_q E_m^{q+4} \left\{ \frac{6q!}{(q+4)!} (1 - (1-x)^{q+4}) - \frac{3}{q+1} \left(\frac{x^{q+2}}{q+2} - \frac{2x^{q+3}}{q+3} + \frac{x^{q+4}}{q+4} \right) \right\} \right\rangle \quad (4.14)$$

Boutiche [44] assumed that:

$$m(\text{Ei}) = m_0(\text{Ei}) + \mu(E_i, q) \quad (4.15)$$

Where $m_0(\text{Ei})$ represent the number of conductances resulting from the symmetrical

part $N(E_F)$ of the density of states $N(E)$ (first *dimension-i*) and $\mu(E_i, q)$ is the number of conductances resulting from the asymmetrical part of $N(E)$ (*second dimension-j*).

By comparing equations (4.14) and (4.15), we obtain for $E_i > 0$:

$$m_0(x) = \frac{2\pi}{3} \frac{N(E_F)}{(2\alpha kT)^3} E_m^4 (1+x)(1-x)^3 \quad (4.16)$$

And,

$$\mu(x, q) = \frac{4\pi}{3} \frac{N(E_F)}{(2\alpha kT)^3} \frac{E_m^{q+4}}{E_0^q} \left\{ \frac{6q!}{(q+4)!} (1-(1-x)^{q+4}) - \frac{3}{q+1} \left(\frac{x^{q+2}}{q+2} - \frac{2x^{q+3}}{q+3} + \frac{x^{q+4}}{q+4} \right) \right\} \quad (4.17)$$

Where $v_q = 1/E_0^q$ and E_0 is the energy solution of the equation $N(E) = 0$.

In equations (4.16) and (4.17) replace x by $-x$ to get the following two expressions for $m_0(x)$ and $\mu(x, q)$ when $E_i < 0$:

$$m_0(x) = \frac{2\pi}{3} \frac{N(E_F)}{(2\alpha kT)^3} E_m^4 (1-x)(1+x)^3 \quad (4.18)$$

$$\mu(x, q) = \frac{4\pi}{3} \frac{N(E_F)}{(2\alpha kT)^3} \frac{E_m^{q+4}}{E_0^q} \left\{ \frac{6q!}{(q+4)!} (-1+(1+x)^{q+4}) - \frac{3}{q+1} \left(\frac{x^{q+2}}{q+2} + \frac{2x^{q+3}}{q+3} + \frac{x^{q+4}}{q+4} \right) \right\} \quad (4.19)$$

Since $m(x)$ is a physical product of the density of states and q is an odd number we have $m_0(-x) = m_0(x)$ and $\mu(-x, q) = -\mu(x, q)$.

The last step of the resolution of Boutiche [44] percolation problem concerns the evaluation of the average number (c) of conductances linked to the site located at energy E_i . To obtain this number we follow the method of Pollak [45], he assumed that c is proportional to $m(E_i)$ by a proportionality factor $N(E_i)$. So,

$$c = \frac{\int_{-E_m}^{E_m} m(E_i)^2 N(E_i) dE_i}{\int_{-E_m}^{E_m} m(E_i) N(E_i) dE_i} = \frac{\int_{-1}^1 m(x)^2 N(x) dx}{\int_{-1}^1 m(x) N(x) dx} \quad (4.20)$$

Then expand their integrands under the form:

$$c = \frac{\int_{-1}^1 (m_0(x) + \mu(x, q))^2 (1 + v_q(x)) dx}{\int_{-1}^1 (m_0(x) + \mu(x, q)) (1 + v_q(x)) dx} \quad ; \quad \text{Where } v_q(x) = E_m^q v_q x^q$$

$$\text{So, } c = \frac{\int_{-1}^1 \{ (m_0(x)^2 + \mu(x, q)^2) + 2m_0(x)\mu(x, q) \} (1 + v_q(x)) dx}{\int_{-1}^1 (m_0(x) + \mu(x, q)) (1 + v_q(x)) dx}$$

$$\text{Then, } c = \frac{\int_{-1}^1 [m_0(x)^2 + \mu(x, q)^2 + 2m_0(x)\mu(x, q)v_q(x)] dx}{\int_{-1}^1 [m_0(x) + \mu(x, q)v_q(x)] dx} \quad (4.21)$$

In equation (4.21) we have to write the asymmetrical functions since their integrations cancel over positive and negative energies. In equation (4.21) we can neglect all terms containing $\mu(x, q)$ since the surface which is determined by these terms is negligible in comparison with the one corresponding to $m_0(x)^2$ when $q \geq 1$.

In such a situation, equation (4.21) becomes quasi similar to the one found in [45] for a constant DOS.

$$c = \frac{\int_{-1}^1 m_0(x)^2 dx}{\int_{-1}^1 m_0(x) dx} \quad (4.22)$$

Integrating the equation (4.22) and taking as Polak [45] $c=1.7$.

$$c = \frac{2\pi}{3} \frac{N(E_F)}{(2\alpha kT)^3} E_m^4 \frac{\int_{-1}^1 \left((1-x)(1+x)^3 \right)^2 dx}{\int_{-1}^1 (1-x)(1+x)^3 dx}$$

$$c = \frac{2\pi}{3} \frac{N(E_F)}{(2\alpha kT)^3} E_m^4 \frac{\int_{-1}^1 (1-4x+4x^2+4x^3-10x^4+4x^5+4x^6-4x^7+x^8) dx}{\int_{-1}^1 (1-2x+2x^3-x^4) dx}$$

$$c = \frac{2\pi}{3} \frac{N(E_F)}{(2\alpha kT)^3} E_m^4 \frac{\left[x-2x^2+\frac{4}{3}x^3+x^4-2x^5+\frac{2}{3}x^6+\frac{4}{7}x^7-\frac{x^8}{2}+\frac{x^9}{9} \right]_{-1}^1}{\left[x-x^2+\frac{x^4}{2}-\frac{x^5}{5} \right]_{-1}^1}$$

$$1.7 = \frac{\pi}{12} \frac{N(E_F)kT}{\alpha^3} \left(\frac{E_m}{kT} \right)^4 \frac{\left[\frac{384}{189} \right]}{\left[\frac{8}{5} \right]} \quad (4.23)$$

By using the value of T_0 , where $T_0 = \left(\frac{\alpha^3 \lambda}{kN(E_f)} \right)$ and inserting that in equation

(4.23), we obtain: $\frac{E_m}{kT} = 1.5 \left(\frac{T_0}{T} \right)^{\frac{1}{4}}$, where $\lambda \approx 18.2$ (chapter two).

We can then deduce that the hopping energy layer of equation (4.7): $E_m = kT(T_0/T)^{1/4}$ and equation (4.4) are valid for any odd q (and s_q) when $N(E)$ is given by equation (4.4) [44], as if $N(E) = N(E_F)$.

4.2 The exponential DOS:

In this section we consider that the DOS at Fermi level is given by $N_0 \exp\left(\frac{-E_f}{E_0}\right)$,

and the DOS in exponential case [46]:

$$N(E) = N_0 \exp\left(\frac{-E - E_f}{E_0}\right) \quad (4.24)$$

Where $E_0 = kT$, and N_0 is the pre-exponential constant, and write $N(E_i)$ as

$$N(E_i) = N_f \exp\left(\frac{-E_i}{E_0}\right), \text{ where } N_f = N_0 \exp\left(\frac{-E_f}{E_0}\right). \quad (4.25)$$

To calculate $m(E_i)$ the two critical conditions which are mentioned in the previous section must be satisfied, see relation (4.5) and equation (4.6). Indeed, we will follow the same technique as in the prior section to evaluate $m(E_i)$. Now from equation (4.10) and equation (4.25) we can write $m(E_i)$ as follows:

$$m(E_i) = \frac{4\pi}{3} \frac{N_f}{(2\alpha kT)^3} \left\{ \int_0^{E_i} (E_m - E_i)^3 \exp\left(\frac{-E_j}{E_0}\right) dE_j + \int_{E_i}^{E_m} (E_m - E_j)^3 \exp\left(\frac{-E_j}{E_0}\right) dE_j \right. \\ \left. + \int_{-(E_m - E_i)}^0 (E_m - E_i + E_j)^3 \exp\left(\frac{-E_j}{E_0}\right) dE_j \right\}$$

Let us denote the integrals in the last expression as H_1, H_2 and H_3 , then

$$m(E_i) = \frac{4\pi}{3} \frac{N_f}{(2\alpha kT)^3} (H_1 + H_2 + H_3).$$

By elementary calculations we can evaluate H_1, H_2 and H_3 as follows:

$$H_1 = -E_0 (E_m - E_i)^3 \left[\exp\left(\frac{-E_i}{E_0}\right) - 1 \right]$$

Let $x = \frac{E_i}{E_m}$ and $s = \frac{E_m}{E_0}$, then

$$\mathbf{H}_1 = E_0^4 s^3 (x-1)^3 [\exp(-sx) - 1] \quad (4.26)$$

$$\begin{aligned} \mathbf{H}_2 &= \int_{E_i}^{E_m} (E_m - E_j)^3 \exp\left(\frac{-E_j}{E_0}\right) dE_j = \int_{E_i}^{E_m} (E_m^3 - 3E_m^2 E_j + 3E_m E_j^2 - E_j^3) \exp\left(\frac{-E_j}{E_0}\right) dE_j \\ \mathbf{H}_2 &= E_m^3 \int_{E_i}^{E_m} \exp\left(\frac{-E_j}{E_0}\right) dE_j - 3E_m^2 \int_{E_i}^{E_m} E_j \exp\left(\frac{-E_j}{E_0}\right) dE_j + 3E_m \int_{E_i}^{E_m} E_j^2 \exp\left(\frac{-E_j}{E_0}\right) dE_j - \int_{E_i}^{E_m} E_j^3 \exp\left(\frac{-E_j}{E_0}\right) dE_j \end{aligned}$$

Using integration by parts we get:

$$\mathbf{H}_2 = \left[\begin{aligned} & -E_m^3 E_0 \exp\left(\frac{-E_j}{E_0}\right) + 3E_m^2 E_0 (E_j + E_0) \exp\left(\frac{-E_j}{E_0}\right) - 3E_m E_0 (E_j^2 + 2E_j E_0 + 2E_0^2) \exp\left(\frac{-E_j}{E_0}\right) \\ & + E_0 (E_j^3 + 3E_j^2 E_0 + 6E_j E_0^2 + 6E_0^3) \exp\left(\frac{-E_j}{E_0}\right) \end{aligned} \right]_{E_i}^{E_m}$$

$$\mathbf{H}_2 = \left[\exp\left(\frac{-E_j}{E_0}\right) E_0^4 \left\{ -s^3 + 3s^2 \left(\frac{E_j}{E_0} + 1\right) - 3s \left(\frac{E_j^2}{E_0^2} + 2\frac{E_j}{E_0} + 2\right) + \left(\frac{E_j^3}{E_0^3} + 3\frac{E_j^2}{E_0^2} + 6\frac{E_j}{E_0} + 6\right) \right\} \right]_{E_i}^{E_m}$$

$$\begin{aligned} \mathbf{H}_2 &= \exp\left(\frac{-E_m}{E_0}\right) E_0^4 \left\{ -s^3 + 3s^2 \left(\frac{E_m}{E_0} + 1\right) - 3s \left(\frac{E_m^2}{E_0^2} + 2\frac{E_m}{E_0} + 2\right) + \left(\frac{E_m^3}{E_0^3} + 3\frac{E_m^2}{E_0^2} + 6\frac{E_m}{E_0} + 6\right) \right\} \\ &- \exp\left(\frac{-E_i}{E_0}\right) E_0^4 \left\{ -s^3 + 3s^2 \left(\frac{E_i}{E_0} + 1\right) - 3s \left(\frac{E_i^2}{E_0^2} + 2\frac{E_i}{E_0} + 2\right) + \left(\frac{E_i^3}{E_0^3} + 3\frac{E_i^2}{E_0^2} + 6\frac{E_i}{E_0} + 6\right) \right\} \end{aligned}$$

$$\begin{aligned} \mathbf{H}_2 &= \exp(-s) E_0^4 \left\{ -s^3 + 3s^2 (s+1) - 3s (s^2 + 2s + 2) + (s^3 + 3s^2 + 6s + 6) \right\} \\ &- \exp(-sx) E_0^4 \left\{ -s^3 + 3s^2 (sx+1) - 3s (s^2 x^2 + 2sx + 2) + (s^3 x^3 + 3s^2 x^2 + 6sx + 6) \right\} \end{aligned}$$

$$\mathbf{H}_2 = E_0^4 \left(6\exp(-s) - \exp(-sx) \left\{ -s^3 + 3s^2 (sx+1) - 3s (s^2 x^2 + 2sx + 2) + (s^3 x^3 + 3s^2 x^2 + 6sx + 6) \right\} \right) \quad (4.27)$$

And the last integral

$$H_3 = \int_{(E_i-E_m)}^0 (E_j - (E_i - E_m))^3 \exp\left(\frac{-E_j}{E_0}\right) dE_j$$

$$H_3 = \int_{(E_i-E_m)}^0 (E_j^3 - 3E_j^2(E_i - E_m) + 3E_j(E_i - E_m)^2 - (E_i - E_m)^3) \exp\left(\frac{-E_j}{E_0}\right) dE_j$$

$$H_3 = \int_{(E_i-E_m)}^0 E_j^3 \exp\left(\frac{-E_j}{E_0}\right) dE_j - 3(E_i - E_m) \int_{-(E_m-E_i)}^0 E_j^2 \exp\left(\frac{-E_j}{E_0}\right) dE_j \\ + 3(E_i - E_m)^2 \int_{-(E_m-E_i)}^0 E_j \exp\left(\frac{-E_j}{E_0}\right) dE_j - (E_i - E_m)^3 \int_{-(E_m-E_i)}^0 \exp\left(\frac{-E_j}{E_0}\right) dE_j$$

Using integration by parts we get:

$$H_3 = \left[\begin{array}{l} -E_0(E_j^3 + 3E_j^2 E_0 + 6E_j E_0^2 + 6E_0^3) \exp\left(\frac{-E_j}{E_0}\right) + 3E_0(E_i - E_m)(E_j^2 + 2E_j E_0 + 2E_0^2) \exp\left(\frac{-E_j}{E_0}\right) \\ -3E_0(E_i - E_m)^2(E_j + E_0) \exp\left(\frac{-E_j}{E_0}\right) + E_0(E_i - E_m)^3 \exp\left(\frac{-E_j}{E_0}\right) \end{array} \right]_{(E_i-E_m)}^0$$

$$H_3 = \left(-E_0(6E_0^3) + 3E_0(E_i - E_m)(2E_0^2) - 3E_0(E_i - E_m)^2(E_0) + E_0(E_i - E_m)^3 \right) \\ - \exp\left(\frac{-(E_i - E_m)}{E_0}\right) \left(\begin{array}{l} -E_0((E_i - E_m)^3 + 3(E_i - E_m)^2 E_0 + 6(E_i - E_m)E_0^2 + 6E_0^3) \\ + 3E_0(E_i - E_m)((E_i - E_m)^2 + 2(E_i - E_m)E_0 + 2E_0^2) \\ - 3E_0(E_i - E_m)^2((E_i - E_m) + E_0) + E_0(E_i - E_m)^3 \end{array} \right)$$

$$H_3 = E_0^4 \left\{ -6 + 6(sx - s) - 3(sx - s)^2 + (sx - s)^3 \right\} + 6E_0^4 \exp(-(sx - s)) \quad (4.28)$$

Therefore, from equations (4.26- 4.28) we get:

$$H_1 + H_2 + H_3 = E_0^4 \exp(-sx) s^3 (x-1)^3 - E_0^4 s^3 (x-1)^3 \\ + E_0^4 \left(6 \exp(-s) - \exp(-sx) \left\{ -s^3 + 3s^2(sx+1) - 3s(s^2x^2 + 2sx + 2) + (s^3x^3 + 3s^2x^2 + 6sx + 6) \right\} \right) \\ + E_0^4 \left\{ -6 + 6(sx - s) - 3(sx - s)^2 + (sx - s)^3 \right\} + 6E_0^4 \exp(-(sx - s))$$

$$H_1 + H_2 + H_3 = -3E_0^4 \left\{ \exp(-sx) \left((s(x-1)+1)^2 + 1 - 2e^s \right) + \left((s(x-1)-1)^2 + 1 - 2e^{-s} \right) \right\} \quad (4.29)$$

So,

$$m(x) = \frac{4\pi N_f}{(2\alpha kT)^3} E_0^4 \left\{ -\exp(-sx) \left\langle (s(x-1)+1)^2 + 1 - 2e^s \right\rangle - \left\langle (s(x-1)-1)^2 + 1 - 2e^{-s} \right\rangle \right\} \quad (4.30)$$

Now we want to obtain the average number of conductances linked to the site located at energy E_i by weighting $m(E_i)$ with a probability factor that is proportional to $m(E_i).N(E_i)$, so that equation (4.6) becomes:

$$c = \frac{\int_{-1}^1 m(x)^2 N(x) dx}{\int_{-1}^1 m(x) N(x) dx} \quad (4.31)$$

Replace $m(x)$ in equation (4.31) by its value in equation (4.30) and taking in account that the exponential DOS $N(E_i) = N_f \exp\left(\frac{-E_i}{E_0}\right)$ so, $N(x) = N_f \exp(-sx)$, we can write

c as follows:

$$c = \frac{-4\pi N_f}{(2\alpha kT)^3} E_0^4 \frac{\int_{-1}^1 \left\{ -\exp(-sx) \left\langle (s(x-1)+1)^2 + 1 - 2e^s \right\rangle - \left\langle (s(x-1)-1)^2 + 1 - 2e^{-s} \right\rangle \right\}^2 \exp(-sx) dx}{\int_{-1}^1 \left\{ -\exp(-sx) \left\langle (s(x-1)+1)^2 + 1 - 2e^s \right\rangle - \left\langle (s(x-1)-1)^2 + 1 - 2e^{-s} \right\rangle \right\} \exp(-sx) dx} \quad (4.32)$$

To simplify equation (4.32) we let

$$Z = \left\{ -\exp(-sx) \left\langle (s(x-1)+1)^2 + 1 - 2e^s \right\rangle - \left\langle (s(x-1)-1)^2 + 1 - 2e^{-s} \right\rangle \right\} \quad (4.33)$$

Then

$$c = \frac{-4\pi N_f}{(2\alpha kT)^3} E_0^4 \frac{\int_{-1}^1 Z^2 \exp(-sx) dx}{\int_{-1}^1 Z \exp(-sx) dx} = \frac{U_1}{U_2}$$

Elementary calculations give

$$U_1 = \frac{1}{s} \left(2 + e^{-s} - \frac{1}{4} e^{-2s} - 2e^s - 4s^2 e^s - e^{2s} + \frac{3}{2} s e^{2s} - 2s^2 e^{2s} + e^{3s} \right) \quad (4.34)$$

And U_2 ,

$$\begin{aligned} U_2 = \int_{-1}^1 Z^2 e^{-sx} dx &= \int_{-1}^1 e^{-sx} \left[\begin{aligned} &(4 + 8s + 8s^2 + 4s^3 + s^4 - 8e^{-s} - 8se^{-s} - 4s^2 e^{-s} + 4e^{-2s}) \\ &+ x(-8s - 16s^2 - 12s^3 - 4s^4 + 8se^{-s} + 8s^2 e^{-s}) \\ &+ x^2(8s^2 + 12s^3 + 6s^4 - 4s^2 e^{-s}) + x^3(-4s^3 - 4s^4) + x^4 s^4 \end{aligned} \right] dx \\ &+ 2 \int_{-1}^1 e^{-2sx} \left[\begin{aligned} &(8 + s^4 - 4e^{-s} + 4se^{-s} - 2s^2 e^{-s} - 4e^s - 4se^s - 2s^2 e^s) \\ &+ x(4s^4 - 4se^{-s} + 4s^2 e^{-s} + 4se^s + 4s^2 e^s) \\ &+ x^2(6s^4 - 2s^2 e^{-s} - 2s^2 e^s) + x^3(-4s^4) + x^4 s^4 \end{aligned} \right] dx \\ &+ \int_{-1}^1 e^{-3sx} \left[\begin{aligned} &(4 - 8s + 8s^2 - 4s^3 + s^4 - 8e^s + 8se^s - 4s^2 e^s + 4e^{2s}) \\ &+ x(8s - 16s^2 + 12s^3 - 4s^4 - 8se^s + 8s^2 e^s) \\ &+ x^2(8s^2 - 12s^3 + 6s^4 - 4s^2 e^s) + x^3(4s^3 - 4s^4) + x^4 s^4 \end{aligned} \right] dx \end{aligned} \quad (4.35)$$

Thus,

$$U_2 = \frac{1}{s} \left\{ \begin{aligned} &-e^{-s}(12 - 8e^{-s} + 4e^{-2s}) + e^s(12 - 16s + 32s^2 + 16s^4 - 8e^{-s} - 16s^2 e^{-s} + 4e^{-2s}) \\ &-e^{-2s} \left(\frac{13}{2} + 3s + 4s^3 + 8s^4 - 7e^{-s} - 3e^s \right) \\ &+ e^{2s} \left(\frac{13}{2} - 3s + 12s^2 - 12s^3 + 8s^4 - 7e^{-s} + 12se^{-s} + 8s^2 e^{-s} - 3e^s - 4se^s - 8s^2 e^s \right) \\ &-e^{-3s} \left(\frac{280}{81} - \frac{104}{27} e^s + \frac{4}{3} e^{2s} \right) \\ &+ e^{2s} \left(\frac{280}{81} - \frac{80}{9} s + \frac{160}{9} s^2 - \frac{80}{9} s^3 + \frac{16}{3} s^4 - \frac{104}{27} e^s + \frac{64}{9} se^s - \frac{16}{3} s^2 e^s + \frac{4}{3} e^{2s} \right) \end{aligned} \right\} \quad (4.36)$$

Therefore,

$$c = \frac{4\pi N_f}{(2\alpha kT)^3} E_0^4 \left\{ \begin{array}{l} e^{-s} (12 - 8e^{-s} + 4e^{-2s}) \\ - e^s (12 - 16s + 32s^2 + 16s^4 - 8e^{-s} - 16s^2 e^{-s} + 4e^{-2s}) \\ + e^{-2s} \left(\frac{13}{2} + 3s + 4s^3 + 8s^4 - 7e^{-s} - 3e^s \right) \\ - e^{2s} \left(\frac{13}{2} - 3s + 12s^2 - 12s^3 + 8s^4 - 7e^{-s} \right. \\ \left. + 12se^{-s} + 8s^2 e^{-s} - 3e^s - 4se^s - 8s^2 e^s \right) \\ + e^{-3s} \left(\frac{280}{81} - \frac{104}{27} e^s + \frac{4}{3} e^{2s} \right) \\ - e^{2s} \left(\frac{280}{81} - \frac{80}{9} s + \frac{160}{9} s^2 - \frac{80}{9} s^3 + \frac{16}{3} s^4 \right) \\ \left. - \frac{104}{27} e^s + \frac{64}{9} se^s - \frac{16}{3} s^2 e^s + \frac{4}{3} e^{2s} \right\} \div \left\{ \begin{array}{l} 2 + e^{-s} - \frac{1}{4} e^{-2s} - 2e^s - 4s^2 e^s \\ - e^{2s} + \frac{3}{2} se^{2s} - 2s^2 e^{2s} + e^{3s} \end{array} \right\}$$

From the last expression it is very difficult to find c analytically, so we move to the numerical way to see the validity of the hopping energy $E_m = kT(T_0/T)^{1/4}$ when $N(E)$ is given by equation (4.22). To that we compare between the curves of the polynomial DOS and the exponential DOS, equations (4.15) and (4.30) respectively, as q goes to 0 and then find the value of E_m at the best correlation, (see Figure 8, Table 9).

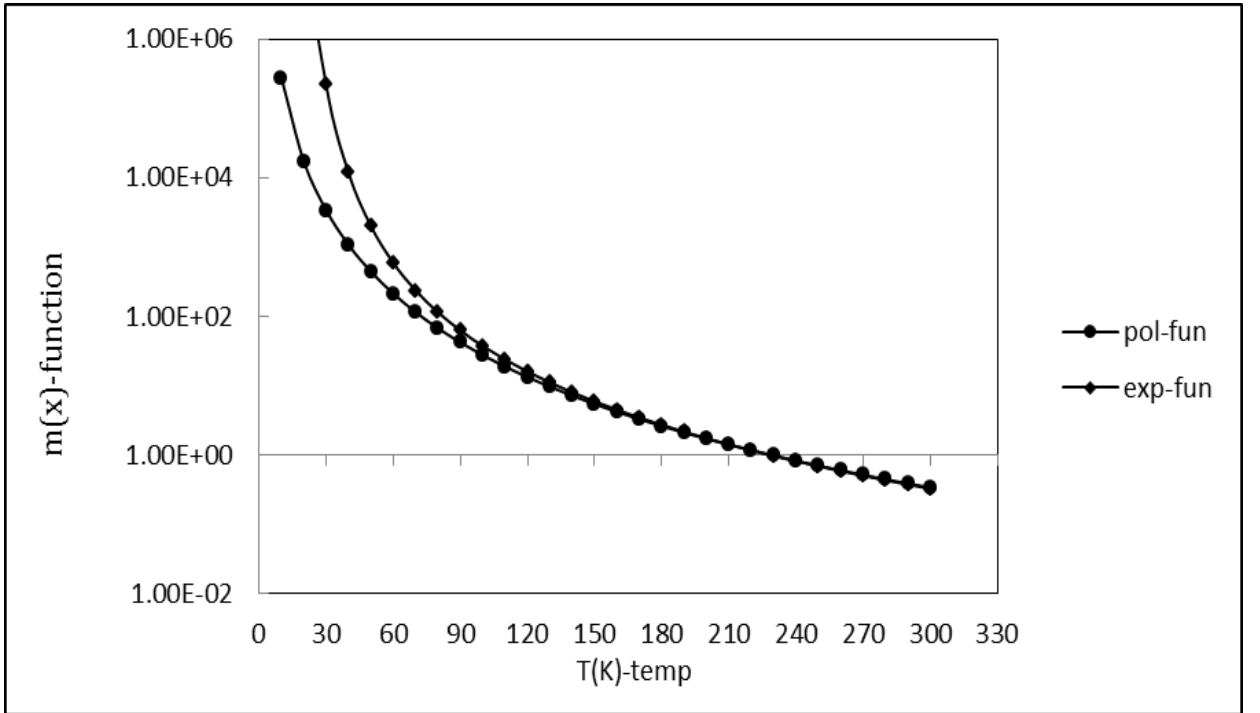


Figure8: Plot of the best correlation of $m(x)$ number of conductances between polynomial DOS ($\lim q \rightarrow 0$) and exponential DOS (with $E_m = 0.08eV$ and $E_i = 0.008eV$ attached to the temperature T(10 K-300 K).

Table 9: : the value of E_m with many correlation of fitting between $m(x)$ function in polynomial DOS ($\lim q \rightarrow 0$) and exponential DOS with $E_i = 0.008eV$.

$E_m(E_i=0.008eV)$	Correlation	Range of T (K)
0.03	0.62	60-300
0.035	0.67	70-300
0.04	0.72	90-300
0.045	0.75	110-300
0.05	0.78	130-300
0.055	0.82	150-300
0.06	0.85	180-300
0.065	0.88	200-300
0.07	0.91	230-300
0.075	0.95	260-300
<u>0.08</u>	<u>0.98</u>	<u>280-300</u>

Conclusions

The derivation and simulation of variable range hopping transport theory was carried out to check the validity of the theory for variable density of localized states near the Fermi level. The conclusions are: The hopping transport is easily controllable via photoexcitation as shown in Figure 2, the photoexcitation can reduce the hopping energy and the hopping range, that means wider distances for electrons to move via photoexcitation, also the higher the light intensity, the less the degree of disorder, the low heat and energy consumption as shown in Figure 6, 7(a, b). Even though Mott derive his theory assuming constant density of localized states, it is still correct for variable polynomial and exponential types of DOS when extra light energy is supplied to the moving electrons.

These analyses are promising as they may support faster random access memories and lower energy consumptions

Appendix A

Curve Fitting by Microsoft Excel to approximate the value of λ

Step1: input the experimental data to calculate the values of T_0 and σ_2 as in table 2.

Step2: Evaluate $N(E_F)$ using equation 3.1; we call this value the actual value.

Step3: Create names for λ . Input the initial values for λ (e.g., 1). Then click on **Insert, Name, and Create**. Then a new window will pop up and just click ok.

Step4: Predict $N(E_F)$ using the assumed value of λ in step3 via equation 3.2.

Step5: Compute the square of the difference between the actual value and the predicted value.

Step6: Compute the sum the square of the differences by using the **AutoSum** button.

Step7: Click on **Tools, Solver**, Set the sum of diff^2 cell as our Target Cell (the sum of the square of the differences = variance). Now make the target cell Equal to **Min. By Changing Cells**, select the cells where the numeric value of T_0 are located. Now you can click on **Solve** and Excel will minimize the difference between the predicted $N(E_F)$ and actual $N(E_F)$ by

Changing the value of λ . A new window will popup after you click solve, just click **OK**.

Step8: Plot both the actual and predicted values in Excel. You can do this by highlighting the light Intensity $F, N(E_F)$ and predicted $N(E_F)$ columns. Then click on the **Chart Wizard** button. Select XY scatter as the chart type and click finish. (See table3)

Step9: Now the actual points are shown in (a) and the predicted values are shown in (b) (in figure 3). Notice the predicted values do not fall exactly on top of the actual strength. This means the predicted values are not good.

Appendix B

Fitting the conduction

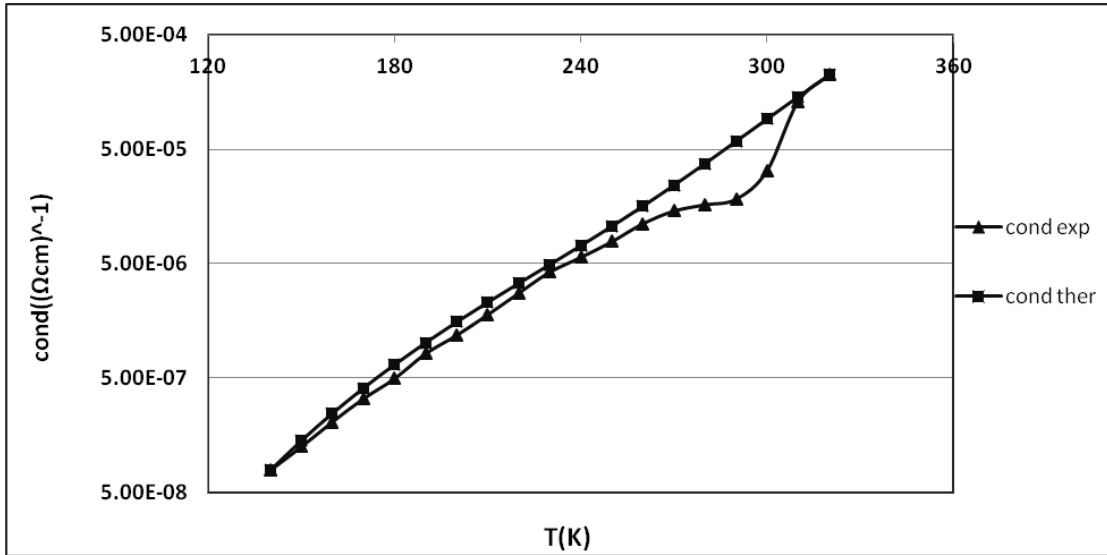


Figure B(1) :fitting conductivity at dark.

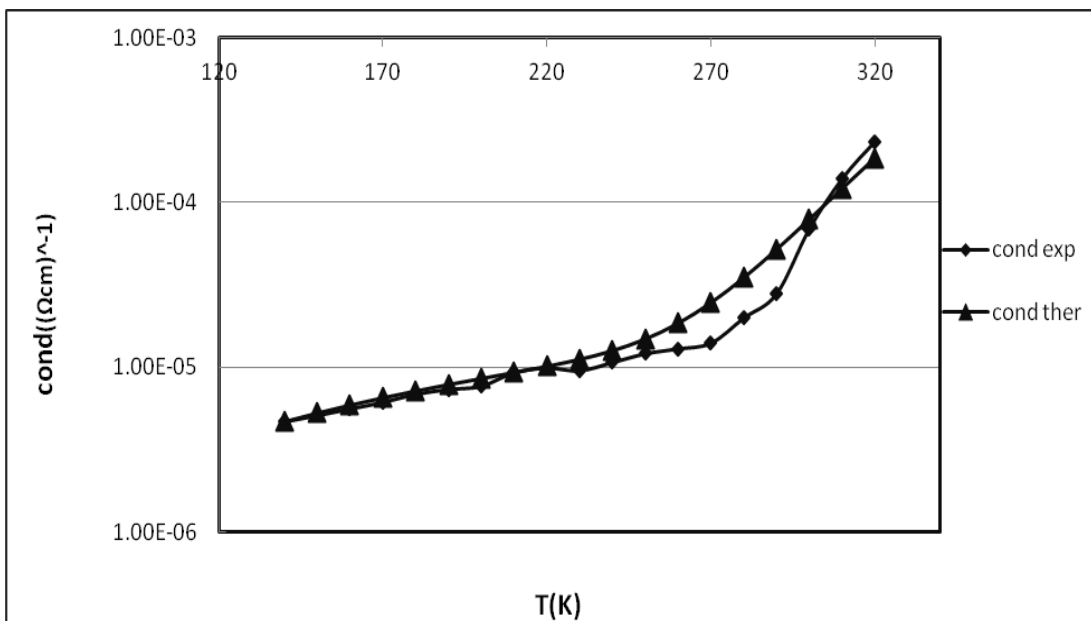


Figure B(2) :fitting conductivity at $F=50 \text{ (mW.cm}^{-2}\text{)}$.

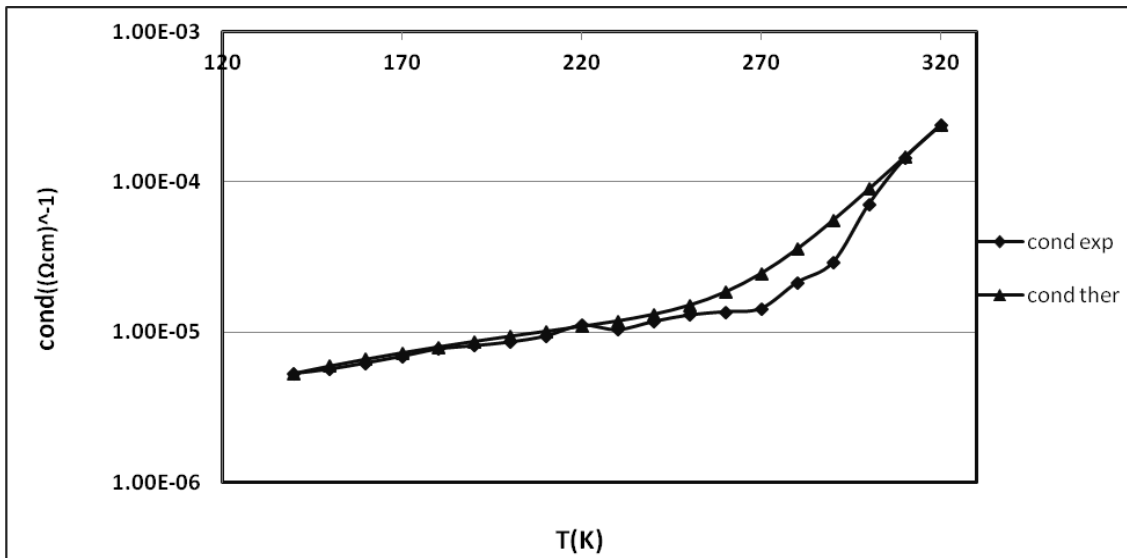


Figure B(3): fitting conductivity at $F=55 \text{ (mW.cm}^{-2}\text{)}$

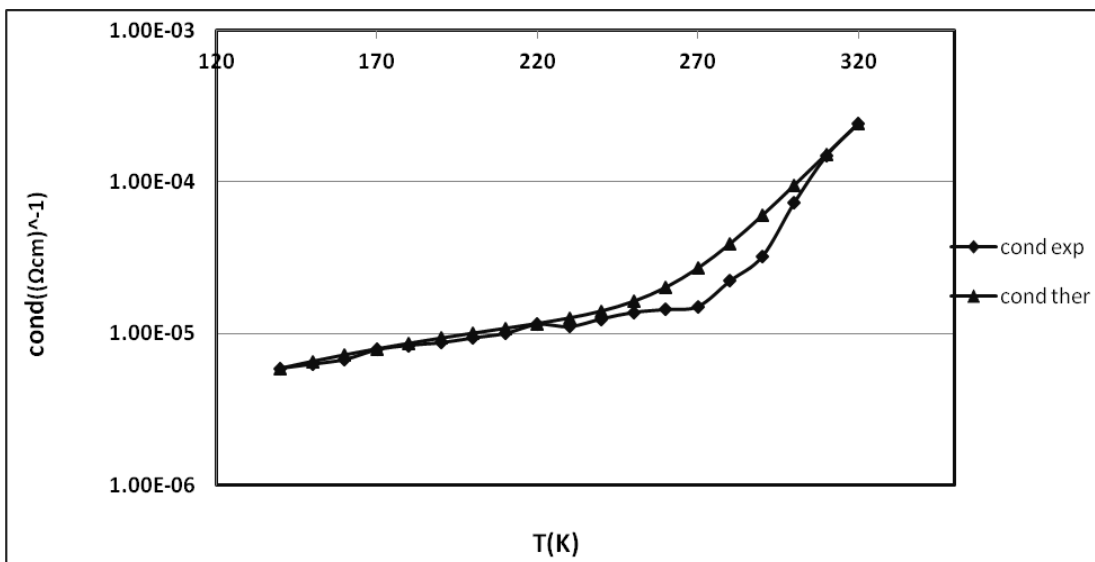


Figure B(4): fitting conductivity at $F=60 \text{ (mW.cm}^{-2}\text{)}$.

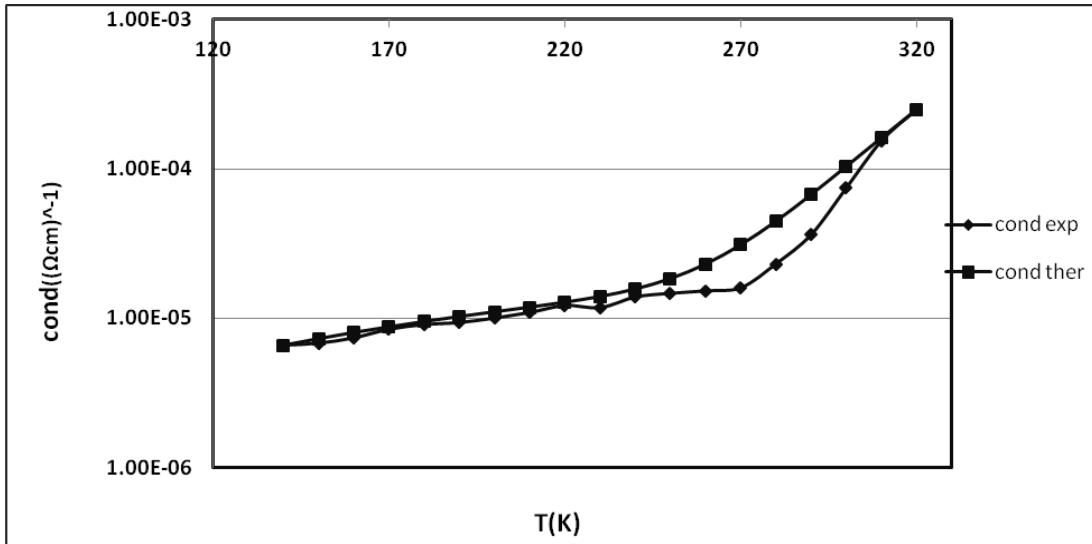


Figure B(5) :fitting conductivity at $F=65 \text{ (mW.cm}^{-2}\text{)}$.

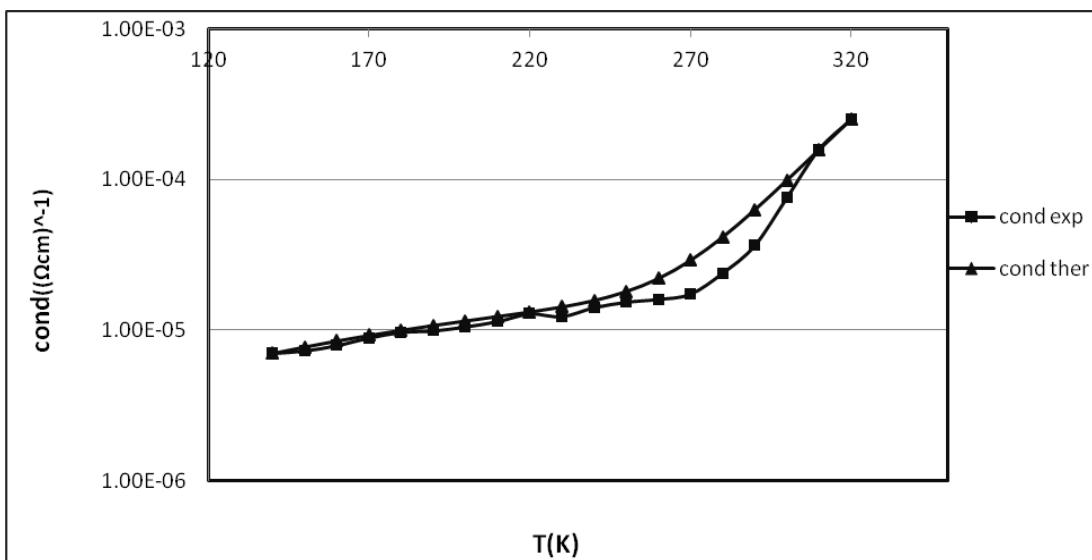


Figure B(6): fitting conductivity at $F=70 \text{ (mW.cm}^{-2}\text{)}$.

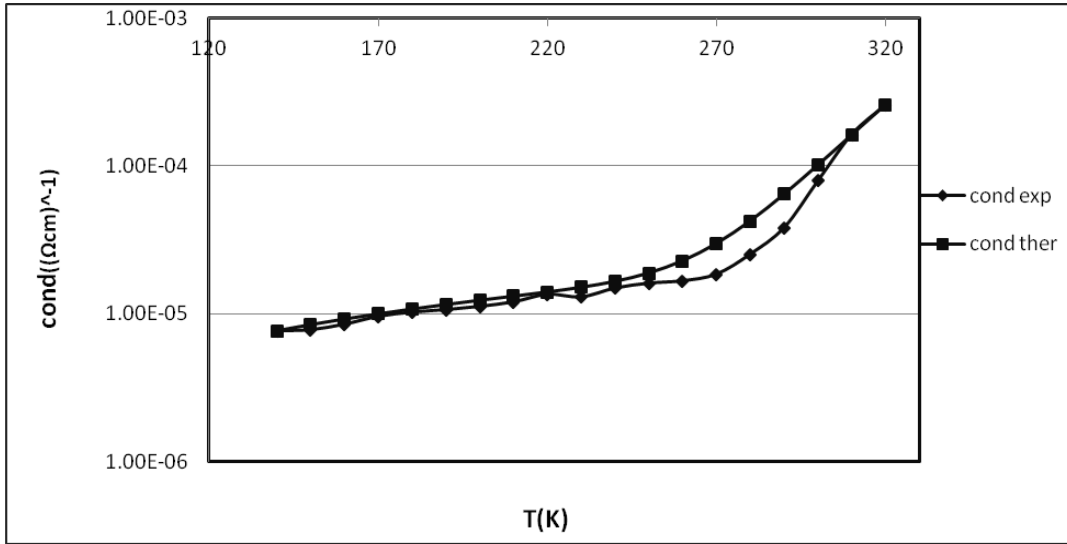


Figure B(7): fitting conductivity at $F=75 \text{ (mW.cm}^{-2}\text{)}$.

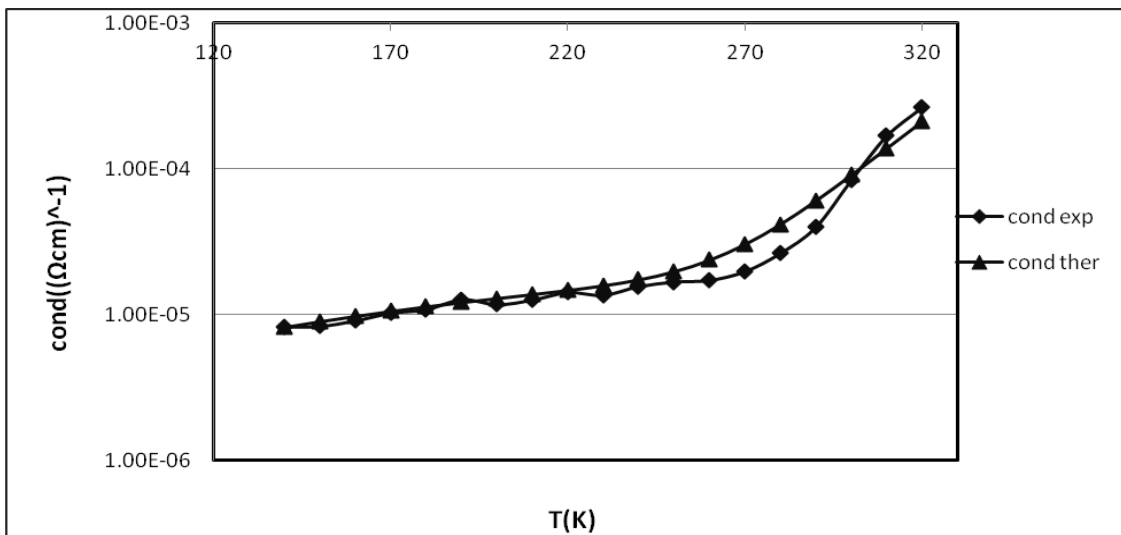


Figure B(8): fitting conductivity at $F=80 \text{ (mW.cm}^{-2}\text{)}$.

References

- [1] E. M Conwell, Impurity Band Conduction in Germanium and Silicon, *Phys. Rev*103, 51, 1956.
- [2] N.F. Mott, Conduction in non-crystalline materials, localized states in a pseudo gap and near extremities of conduction and valence bands on crystalline materials, localized states, *Philosophical Magazine*, 19:835–852, 1969.
- [3] E. Abrahams, A. Miller, Impurity conduction at low concentrations, *Physical Review*, 120, 1960.
- [4] P.W. Anderson, Absence of Diffusion in Certain Random Lattices, *Phys. Rev* 109, 1492, 1958.
- [5] M. Ortuno, J. Talamantes, E. Cuevas, A. Diaz-Sanchez, Coulomb interactions in Anderson insulators. *Philosophical Magazine B*, 81(9):1049–1064, 2001.
- [6] I. P. Zvyagin, On the Theory of Hopping Transport in Disordered semi- conductors, *Physica Status Solidi (b)*, vol.58, 443, 1973.
M. Pollak., and B. Shklovskii., *Hopping Transport in Solids*, 143, 1991.
- [7] A. L. Efros, B. I. Sklovskii, *Electronic Properties of Doped Semiconductors*, Springer-Verlag, Berlin Heidelberg, New York, Tokyo, 1984.
- [8] P.V.E. McClintock, D. J. Meredith, J. K. Wigmore, *Matter at low Temperature*, Blackie, ISBN 0-216-91594-5, 1984.
- [9] L Pichon, E Jacques, R Rogel, A C Salaun, F Demami, variable range hopping conduction in N- and P-type in situ doped poly crystalline silicon nano-wires, *SemiCond. Sci. Technol.* 28, 025002, 2013.
- [10] K. Huang Chen, R. Zhang, T. Chang, T. Ming Tsai; K. Chang, hopping conduction distance dependent activation energy characteristics of Zn:SiO₂ resistance random access memory devices, *Appl. Phys. Lett.*, 102,133503, 2013.
- [11] E. Song; J. Woo Choi, Conducting polyaniline nanowire and its applications in chemiresistive Sensing, *non-materials*, 3, 498-523, 2013.
- [12] S. Virji, R.B. Kaner, B.H. Weiller, Hydrogen sensors based on conductivity changes in polyaniline nanofibers, *J. Phys. Chem. B*, 110, 22266–22270, 2006.
- [13] J. Wang, Y.L. Bunimovich, G. Sui, S. Savvas, J. Wang, Y. Guo, J.R Heath, H. Tseng, R-Electrochemical fabrication of conducting polymer nanowires in an integrated microfluidic system, *Chem. Commun.*, 29, 3075–3077, 2006.

[14] Y. Cao, P. Smith, A. J. Heeger, Counter-Ion Induced Processibility of Conducting Polyaniline and of Conducting Polyblends of Polyaniline in Bulk Polymers, *Synthetic Metals*, Vol. 48, No. 1, pp. 91-97. doi:10.1016/0379-6779(92)90053-L, 1992.

[15] N. Chandrakanthi, M. A. Careem, Preparation and Characterization of Fully Oxidized Form of Polyaniline, *Polymer Bulletin*, Vol. 45, No. 2, pp. 113-120. doi:10.1007/s002890070038, 2000.

[16] K. Roy, J. Bera, Enhancement of the magnetic properties of Ni–Cu–Zn ferrites with the substitution of a small fraction of lanthanum for iron, *Mater. Res. Bull.*, 42, 77,83, 2007.

C. P. Poole, H. A. Farach, Magnetic phase diagram of spinel spin-glasses, *Z. Phys. B.*, 47, 55-57, 1982.

E. J. W. Verwey, J. H. deBoer, Cation arrangement in a few oxides with crystal structures of the spinel type, *Rec. Trav. Chim. Pays. Bas.*, 55, 531-540, 1936.

[17] M. J. M. Lope, M. P. B. Pena, M. E. G. Clavel, The composition of magnesium titanates as a function of the synthesis methods, *Therm. Acta.*, 194, 247-252, 1992.

[18] H. Hohl, C. Kloc, E. Bucher, Electrical and Magnetic Properties of Spinel Solid Solutions, *J. of Solid State Chem.*, 125, 216-223, 1996.

[19] M. Okutan, H. I. Bakan, K. Korkmaz, F. Yakuphanoglu, Variable range hopping conduction and microstructure properties of semiconducting Co-doped TiO₂, *Phys. B.*, 355, 176-181, 2005.

W. A. Badawy, R. S. Momtaz, E. M. Elgiar, Solid State Characteristics of Indium-Incorporated Titanium Dioxide (TiO₂), *Thin Films*, *Phys. Stat. Sol. (A)*, 118, 197-202, 1990.

[20] J. L. Liu, 'Poisson's Equation in Electrostatics', Department of Applied Mathematics, National Hsinchu University of Education, 2011.

[21] L.D. Landau, E.M. Lifshitz, *Statistical Physics, Course of Theoretical Physics 5* (3 ed.), Oxford: Pergamon Press, ISBN 0-7506-3372-7, 1976.

[22] J. W. Gibbs, *Elementary Principle in Statistical Machines*, New York: Charles Scribner's Sons, 1902.

[23] W. Gautschi. "Some elementary inequalities relating to the gamma and incomplete gamma function," *J. Math. Phys.* v. 38, p. 77-81, 1959.

- [24] R. Courant, *Differential and Integral Calculus* (2 volumes), English translation by E. J. McShane, Interscience Publishers, New York, 1961.
- [25] D. Widder, *Advanced Calculus*, 2nd edition, Prentice Hall, 1961.
- [26] M. Godefroy, *The Gamma Function; Theory, History, Bibliography*, Gauthier, Villars, Paris, 1901.
- [27] Z. Dilli, 'Intrinsic and Extrinsic Semiconductors, Fermi-Dirac Distribution Function, the Fermi level and carrier concentrations', Oct. 2008, rev. Mar 2009.
- [28] A. L. Reimann, 'thermionic emission', page 1, Chapman and hall, Ltd., 1934.
- [29] S.R. Broadbent, J.M. Hammersley, *Percolation processes. I. Crystals and Mazes*, *Proceedings of the Cambridge Philosophical Society* 53, 629–641, 1957.
- [30] B. Berkowitz, R. Ewing, *percolation Theory and Network Modeling Applications in Soil Physics*, *Surveys in Geophysics* 19(1), 23-72, 1998.
- [31] P.Z. Wong, *The statistical physics of sedimentary rock*, *Physics Today* 41, 24–32, 1984.
- [32] I. Balberg, *Recent developments in continuum percolation*, *Philosophical Magazine* 56, 991–1003, 1987.
- [33] P. Shing, B. Abeles, Y. Arie, *Hopping Conductivity in Granular materials*, *Physical Review Letters*, volume 31, no.1, 1973.
- [34] B. Bollabas, O. Riordan, *a modern treatment of percolation (The introduction)*, *Percolation*, Cambridge University Press, 2006.
- [35] G. Grimmett, *The slandered reference on percolation (the first two chapters)*, *Percolation*, second edition, 1999.
- [36] N. F. Mott, *The hall effect near The Metal-insulator transitions*, Taylor & Francis, *Journ. Non-cryst. Sol.* 7,1, 1972.
- [37] C. Godet, B. Equer, D. Mencaraglia, *19th International Conference on Amorphous and Microcrystalline Semiconductors*, *Non-Cryst. Solids* 299-302 333, 2002.

- [38] H. P. Apsley, N. Hughes, Temperature- and field-dependence of hopping conduction in disordered systems, *Phil. Mag.* 30: 963, 1974.
- [39] J. Y. W. Seto, The electrical properties of polycrystalline silicon films, *J. appl. phys.* 46, 5247, 1975.
- [40] D. K. Paul, S.S. Mitra, Evaluation of Mott's Parameters for Hopping Conduction in Amorphous Ge, Si, and Ge-Si, *Phys. Rev. Lett.* 13 1000, 1973.
- [41] S. B. Concari, R. H. Buitrago, Proceedings of the 20th International Conference on Amorphous and Microcrystalline Semiconductors, *J. Non-Cryst. Solids* 338-340 331, 2004.
- [42] S. B. Concari, R. H. Buitrago, M. T. Gutierrez, J. Gandia, Electric transport mechanism in intrinsic and p-doped microcrystalline silicon thin films, *J. Appl. Phys.* 94 2417, 2003.
- [43] G. Ambrosone, U. Coscia, A. Cassinese A, M. Barra, S. Restello, V. Rigato, S. Ferrero, *Thin Solid Films* 515 7629, 2007.
- [44] S. Boutiche, Variable Range Hopping Conductivity: Case of the non-constant density of states, Dept. de Physique, Universite de Bechar 08000, Bechar – Algeria, 2009.
- [45] M. Pollak, A percolation treatment of dc hopping conduction, *Journ. Non-cryst. Sol.* 11, 1, p.1-24, 1972.
- [46] L. Pichon, R. Rogel, experimental validation of the exponential localized states distribution in the variable range hopping mechanism in disordered silicon films, 2011
- [47] L. Ling, Charge Transport in Organic Semiconductor Materials and Devices, eingereicht an der Technischen University Wien Fakultät für Elektrotechnik und Informationstechnik von, PHD desertation, (2007).
- [48] B.I. Shklovskii, A.L. Efros, Electronic properties of doped semiconductors, Springer, Heidelberg, 1984.

